AGU ADVANCING EARTH AND SPACE SCIENCES

JAMES | Journal of Advances in Modeling Earth Systems®

RESEARCH ARTICLE
10.1029/2022MS003464

Toward Robust Parameterizations in Ecosystem-Level Photosynthesis Models

Shanning Bao[1,2], Lazaro Alonso[1], Siyuan Wang[1], Johannes Gensheimer[1], Ranit De[1], and Nuno Carvalhais[1,3,4]

[1]Department for Biogeochemical Integration, Max-Planck-Institute for Biogeochemistry, Jena, Germany, [2]National Space Science Center, Chinese Academy of Sciences, Beijing, China, [3]Departamento de Ciências e Engenharia do Ambiente, DCEA, Faculdade de Ciências e Tecnologia, FCT, Universidade Nova de Lisboa, Caparica, Portugal, [4]ELLIS Unit Jena, Jena, Germany

Abstract In a model simulating dynamics of a system, parameters can represent system sensitivities and unresolved processes, therefore affecting model accuracy and uncertainty. Taking a light use efficiency (LUE) model as an example, which is a typical approach for estimating gross primary productivity (GPP), we propose a Simultaneous Parameter Inversion and Extrapolation approach (SPIE) to overcome issues stemming from plant-functional-type (PFT)-dependent parameterizations. SPIE refers to predicting model parameters using an artificial neural network based on collected variables, including PFT, climate types, bioclimatic variables, vegetation features, atmospheric nitrogen and phosphorus deposition, and soil properties. The neural network was optimized to minimize GPP errors and constrain LUE model sensitivity functions. We compared SPIE with 11 typical parameter extrapolating methods, including PFT- and climate-specific parameterizations, global and PFT-based parameter optimization, site-similarity, and regression approaches. All methods were assessed using Nash-Sutcliffe model efficiency (NSE), determination coefficient and normalized root mean squared error, and contrasted with site-specific calibrations. Ten-fold cross-validated results showed that SPIE had the best performance across sites, various temporal scales and assessing metrics. Taking site-level calibrations as a benchmark (NSE = 0.95), SPIE performed with an NSE of 0.68, while all the other investigated approaches showed negative NSE. The Shapley value, layer-wise relevance and partial dependence showed that vegetation features, bioclimatic variables, soil properties and some PFTs determine parameters. SPIE overcomes strong limitations observed in many standard parameterization methods. We argue that expanding SPIE to other models overcomes current limits and serves as an entry point to investigate the robustness and generalization of different models.

Plain Language Summary Parameters can represent ecosystem properties and sensitivities of ecosystem processes to environmental changes, affecting model accuracy and output uncertainties. Therefore determining parameters is of great importance for applying models. Current ecosystem-level models mostly determine parameters according to biomes. For example, light use efficiency (LUE) models, a typical tool to estimate gross primary productivity (GPP), use plant-functional-type (PFT)-specific parameters. However, PFT-specific parameters cannot represent the spatial variance of GPP sensitivities to environmental conditions within PFT and introduce significant estimation errors. To overcome these issues, we propose a Simultaneous Parameter Inversion and Extrapolation method (SPIE). Taking an LUE model as an example, we estimated model parameters using SPIE based on the input features representing vegetation, climate and soil properties at 196 observational sites. We compared SPIE with 11 other parameter extrapolating methods and all of these methods with site-specific calibrations based on full-time-series observed GPP. The results were validated and showed that SPIE was the best method to extrapolate parameters across various temporal and spatial scales. According to the importance of input features, vegetation features, bioclimatic variables, soil properties and some PFTs are dominating spatial changes of parameters. Overall, SPIE is a robust method that overcomes strong limitations in many standard parameter extrapolating methods.

Key Points:

- We propose a machine-learning-based parameterization method to model gross primary productivity
- The method overcomes significant biases in extrapolations using assumptions of biome-dependent and globally fixed parameterizations
- Vegetation, climate and soil properties explain most variability in model parameters, challenging current prescriptions of their patterns

Supporting Information:

Supporting Information may be found in the online version of this article.

Correspondence to:

S. Bao and N. Carvalhais,
sbao@bgc-jena.mpg.de;
ncarvalhais@bgc-jena.mpg.de

Citation:

Bao, S., Alonso, L., Wang, S., Gensheimer, J., De, R., & Carvalhais, N. (2023). Toward robust parameterizations in ecosystem-level photosynthesis models. *Journal of Advances in Modeling Earth Systems*, *15*, e2022MS003464. https://doi.org/10.1029/2022MS003464

Received 17 OCT 2022
Accepted 20 JUL 2023

Author Contributions:

Conceptualization: Shanning Bao, Nuno Carvalhais
Data curation: Shanning Bao
Formal analysis: Shanning Bao
Funding acquisition: Shanning Bao, Siyuan Wang, Johannes Gensheimer, Nuno Carvalhais
Investigation: Shanning Bao
Methodology: Shanning Bao, Lazaro Alonso, Siyuan Wang, Johannes Gensheimer, Ranit De, Nuno Carvalhais

1. Introduction

Increasing studies based on model ensembles reveal that large uncertainties remain in modeling the global carbon cycle and ecosystem responses to environmental changes (Baldocchi et al., 2016; Bloom et al., 2016; Piao et al., 2020). The uncertainties are mainly due to various limitations in model structures, driver data, parameters

Project Administration: Nuno Carvalhais
Resources: Shanning Bao
Supervision: Nuno Carvalhais
Validation: Shanning Bao, Lazaro Alonso, Johannes Gensheimer
Visualization: Shanning Bao
Writing – original draft: Shanning Bao
Writing – review & editing: Lazaro Alonso, Siyuan Wang, Johannes Gensheimer, Ranit De, Nuno Carvalhais

(Huntzinger et al., 2017; Medlyn et al., 2005; Zheng et al., 2018) and a lack of ecological considerations as additional constraints (Bloom & Williams, 2015). Although model parameters contribute to considerable uncertainties, most global vegetation models are parameterized using fixed, biome- or plant functional type (PFT)- based values, which alone cannot capture the spatial variability of carbon assimilation processes (Bloom et al., 2016), arguing for considering aspects related to ecosystem development stage and biodiversity. The fixed and PFT-based parameterization are also widely used and introduced uncertainties in gross primary productivity (GPP) models (Groenendijk et al., 2011; Ryu et al., 2019), including light use efficiency (LUE) models, leaf-scale-process-based models, machine-learning and sun-induced fluorescence models (Frankenberg et al., 2011; Jung et al., 2011; Running et al., 2004; Tian et al., 2020; Zhang et al., 2012). A more robust and physically intuitive parameterization method is desired for constraining the global GPP estimation.

LUE models are typical approaches for the estimation of GPP at large global scales (Mahadevan et al., 2008; Potter et al., 1993; Running et al., 2004; Tian et al., 2020; Yuan et al., 2007). These models incorporate the knowledge of environmental constraints to the originally proposed empirical LUE model, Monteith's model (1972), having the advantages of high efficiency and algorithmic transparency compared to leaf-scale-process-based models and machine-learning-based models, respectively.

The first global GPP product based on the MODIS LUE algorithm (Running et al., 2004) proposed a set of PFT-dependent parameters. Later, other published global LUE models inherited the PFT-based parameterization method or incorporated parameters directly extracted from literature (He et al., 2013; Mahadevan et al., 2008; Xiao et al., 2004; Xie & Li, 2020). The PFT-based approach is not exclusive to LUE models but is also commonly used in dynamic global vegetation models and the land surface schemes of global Earth system models supporting IPCC reports (Ciais et al., 2019; Masson-Delmotte et al., 2021; T. Stocker, 2014; Wenzel et al., 2014). However, applying parameterizations in locations or regions, which have not been previously used or evaluated against observations, might easily lead to naïve conclusions about model structure robustness and/or parameter generalization. To overcome this limitation, LUE models usually calibrate parameters within their physical ranges to minimize the mismatch between the modeled and the observational GPP (Carvalhais et al., 2008; Horn & Schulz, 2011a; Mäkelä et al., 2008; Yan et al., 2017; Zhou et al., 2016), that is, the GPP estimated from eddy covariance (EC) carbon flux. This method is supported by the availability of EC flux towers, given the need for parameter generalization limited for the global domain. To parameterize the Carnegie-Ames-Stanford approach (CASA) model in locations without EC observations, Carvalhais et al. (2010) considered in situ parameterizations from EC sites with the same PFT and similar climate and vegetation features. An alternative approach is to apply globally fixed parameters from literature (Mengoli et al., 2022; H. Wang et al., 2017) or globally optimized parameters (B. D. Stocker et al., 2020; Yuan et al., 2019). Another option to extrapolate parameters is based on clustering approaches. The clustering approaches denote using the average site-level optimized parameters per PFT (Guan et al., 2022; Yuan et al., 2014a; Zhou et al., 2016) or PFT-specific optimized parameters (Tian et al., 2020; Zheng et al., 2020). Yuan et al. (2014b) showed using six different LUE models that the modeled GPP using globally optimized parameters was not significantly different from that using PFT-specific optimized parameters. However, it has been illustrated that at least parameter variations between PFTs need to be considered to reach confident model performances (Tian et al., 2020). In general, most studies did not account for parameter variances within PFT, despite assuming that LUE model parameters are related to characteristics of the vegetation and the environment.

In some studies, the drivers for spatial changes of model parameters were analyzed based on site-level calibrated parameters. For example, Horn and Schulz (2011b) found that their LUE model parameters, which represent the maximum LUE and the sensitivity of GPP to temperature and soil moisture, varied across climate zones and biomes and can be predicted using vegetation and environmental properties. The relationship between parameters and plant traits also existed in process-based GPP models (Peaucelle et al., 2019). Moreover, Luo and Schuur (2020) claimed that model parameters, which can represent both the evolving ecosystem properties and the unresolved ecosystem processes, should be determined according to our knowledge about the changing ecosystem properties. All these studies confirmed the control of vegetation attributes and environmental features on model parameters, which represents GPP sensitivities. These findings inspire the possible next generation of parameterization methods based on the physical connection between model parameters and ecosystem properties.

In this study, we aim to propose a new model parameterization method (or parameter extrapolation method) that explicitly accommodates the contribution of PFT as well as other vegetation features and environmental

conditions to parameter spatial variability. We allow the spatial variation of parameters, indicating GPP sensitivities to environmental forcings, to be learned from a set of ecosystem properties. To test the approach, we compared 12 different parameterization methods (see details in Section 2.2) based on an exemplified LUE model with appropriate environmental drivers and sensitivity functional forms selected from an ensemble of 5600 LUE models (Bao et al., 2022). These parameterization methods were assessed according to the accuracy of the simulated GPP (GPP_{sim}) across different time scales at the site level, per PFT, per climate type and globally (see Section 2.3). The importance of drivers for model parameters was evaluated using three different methods (see Section 2.4).

2. Materials and Methods

2.1. Light Use Efficiency Model

LUE models define GPP as a product between photosynthetically active radiation (PAR), the fraction of absorbed photosynthetically active radiation (FAPAR) and the maximum LUE ($\boldsymbol{\varepsilon_{max}}$), regulated by environmental sensitivity functions. The environmental drivers and sensitivity functional forms, representing the responses from the photosynthesis processes, differ across LUE models and can affect the model's performance. To minimize the selection effect of environmental drivers and sensitivity functions, we select a LUE model based on Bao et al. (2022). The study evaluated a large set of LUE models with various combinations of drivers and functional forms against GPP observations across various PFTs and climate types. The selected model was shown to be the best one compared with those LUE models with different drivers or sensitivity functional forms. In summary, the LUE model considers the impacts of temperature (T), vapor pressure deficit (VPD), atmospheric CO_2 concentration (c_a), soil moisture (W), light intensity (L) and the cloudiness index on GPP dynamics (see Equations 1–8, and Bao et al. (2022)).

$$\mathrm{GPP} = \mathrm{PAR} \cdot \mathrm{FAPAR} \cdot \varepsilon_{\mathbf{max}} \cdot \mathrm{fT} \cdot \mathrm{fVPD} \cdot \mathrm{fW} \cdot \mathrm{fL} \cdot \mathrm{fCI} \tag{1}$$

$$\mathrm{fT} = \frac{2e^{-(T_f - \mathbf{T}_{\mathrm{opt}})/\mathbf{k_T}}}{1 + e^{\left(-(T_f - \mathbf{T}_{\mathrm{opt}})/\mathbf{k_T}\right)^2}} \tag{2}$$

$$\mathrm{fVPD} = e^{\boldsymbol{\kappa}\left(\frac{\mathbf{C_{a0}}}{c_a}\right)^{\mathbf{C}_{\boldsymbol{\kappa}}}\mathrm{VPD}}\left(1 + \frac{c_a - \mathbf{C_{a0}}}{c_a - \mathbf{C_{a0}} + \mathbf{C_m}}\right) \tag{3}$$

$$\mathrm{fW} = \frac{1}{1 + e^{\mathbf{k_W}(\mathbf{W_f} - \mathbf{W_I})}} \tag{4}$$

$$\mathrm{fL} = \frac{1}{1 + \gamma \cdot \mathrm{APAR}} \tag{5}$$

$$\mathrm{fCI} = \mathrm{CI}^{\boldsymbol{\mu}} \tag{6}$$

$$T_f(t) = (1 - \boldsymbol{\alpha_T}) \cdot T(t) + \boldsymbol{\alpha_T} \cdot T_f(t - 1) \tag{7}$$

$$W_f(t) = (1 - \boldsymbol{\alpha_W}) \cdot W(t) + \boldsymbol{\alpha_W} \cdot W_f(t - 1) \tag{8}$$

The LUE model includes 13 parameters in total (in **bold**). All sensitivity functions (i.e., *f*T, *f*VPD, *f*W, *f*L, and *f*CI) are scaled from zero to one, representing from strong to no constraints. The physical meanings and units of the parameters and references of these sensitivity functions are summarized in Table 1.

The sensitivity function of VPD (*f*VPD) includes the effect of both VPD and c_a, which jointly control the leaf internal CO_2 concentration. The pure CO_2 fertilization effect is described only by the right part of *f*VPD (i.e., the sum of one and c_a function). The product of PAR and FAPAR, that is, the absorbed photosynthetically active radiation (APAR), is the estimate of the light energy intercepted by the vegetation canopy, and thus was used as the light intensity input of the sensitivity function of L (*f*L). The T and W were temporally filtered using lag parameters, $\boldsymbol{\alpha_T}$ and $\boldsymbol{\alpha_W}$, at boreal and arid regions, respectively, according to Horn and Schulz (2011a).

2.1.1. Forcing Data and Parameter Calibration

The forcing data for the LUE model was collected at 196 EC sites (listed in Table S1 of the Supporting Information S1) from FLUXNET (www.fluxnet.org). The detailed sources and algorithms of the forcing data are

Table 1
List of Light Use Efficiency Model Parameters

Parameters	Meanings	Range	Units	References
ε_{max}	Maximum light use efficiency	0–10	gC MJ^{-1}	Running et al. (2004)
T_{opt}	Optimal temperature	5–35	°C	Horn and Schulz (2011a)
k_T	Sensitivity to temperature changes	1–20	–	
κ	Sensitivity to vapor pressure deficit changes	-10^{-1} to -10^{-4}	kPa^{-1}	Mäkelä et al. (2008)
C_{a0}	Minimum optimal atmospheric CO_2 concentration	340–390	ppm	Kalliokoski et al. (2018)
C_κ	Sensitivity to atmospheric CO_2 concentration changes	0–10	–	
C_m	CO_2 fertilization intensity indicator	100–4,000	ppm	
k_W	Sensitivity to soil moisture changes	−30 to −5	–	Horn and Schulz (2011a)
W_I	Optimal soil moisture	0.01–0.99	cm cm^{-1}	
γ	Light saturation curvature indicator	0–1	MJ^{-1} m^2 d	Mäkelä et al. (2008)
μ	Sensitivity to cloudiness index changes	10^{-3}–1	–	Bao et al. (2022)
α_T	Lag parameter for temperature effect	0.0–0.9	–	Horn and Schulz (2011a)
α_W	Lag parameter for soil moisture effect	0.0–0.9	–	

summarized in Table S2 of Supporting Information S1. The GPP estimated from the observed net ecosystem exchange at EC sites (GPP_{obs}) were also collected to calibrate parameters and evaluate parameterization methods.

In the parameter calibration process, we added constraints on GPP simulation errors and sensitivity functions (e.g., fT) following the concept of ecological and dynamic constraints (see details in Text S1 of the Supporting Information S1). As a derivative-free global searching algorithm, CMAES (Hansen & Kern, 2004), was used to search the optimal parameters in its physical range according to the full-time series of GPP_{obs}. We assumed that the simulated GPP using the calibrated parameters (GPP_{calib}) can reach the model potential (i.e., the highest model performance). Thus, the performance of the site-level calibrations ("site-calib") was set as the benchmark for other parameterization methods in cross-validation (will be introduced in Section 2.2).

2.1.2. Input Features of Ecosystem Properties for Predicting Model Parameters

To extrapolate the parameters across various sites and in the future to the global scale, we collect mainly the variables that can represent the ecosystem properties available at both local (i.e., site-level) and global scales. These variables include the PFT, climate classification types (Clim; Rubel et al., 2017), 19 bioclimatic variables (BIO1-19, classified as "BioClim"; Xu & Hutchinson, 2011), two aridity features (AI1-2, classified as "BioClim"), 11 vegetation index features (VIF1-11, represented by "VIF"), atmospheric Nitrogen and Phosphorus deposition (NdepNHX, NdepNOY and Pdep, summarized as "NPdep"; R. Wang et al., 2017) and 17 soil properties (classified as "Soil"; Poggio et al., 2021). In other words, we used six classes of input features which are shorted to BioClim, Clim, NPdep, PFT, Soil and VIF. The details of the input features are summarized in Table S3 of Supporting Information S1.

The categorical variables (PFT and climate types) were converted to one or zero to indicate whether the target location belongs to a specific type or not. All non-categorical variables were normalized by subtracting the mean of each feature and dividing by the standard deviation (Equation 9). The original and normalized features are represented by var and var_{nor}. The mean and standard deviation per feature are represented by mean and std, respectively.

$$var_{nor} = \frac{var - mean}{std} \quad (9)$$

2.2. Parameterization Methods

We extrapolate the parameters based on a ten-fold cross-validation strategy using the collected input features. Namely, the samples, referring to the EC sites, were divided into 10 groups randomly (see the group number of

each site in Table S1 of the Supporting Information S1). We trained the parameterization models using nine of 10 groups and validated the result using the one left, and repeated 10 times until we got validated results from all sites. All PFT and climate classification types (11 PFT and 14 climate classification types in total, see Table S1 in Supporting Information S1) were included in each training data set.

The 12 parameterization methods can be divided into six groups, that is, univariate clustering, similarity-based, optimization-based, regression-based, our hybrid approach based on a neural network and globally fixed methods (see details in Sections 2.2.1–2.2.6).

2.2.1. Univariate Clustering Methods ("PFT_{mean}", "$Clim_{mean}$", "PFT_{med}", and "$Clim_{med}$")

In regions without observational data, the parameters were determined by the arithmetic mean from the calibrated parameters at the sites with the same PFT (Guan et al., 2022; Yuan et al., 2014b; Zhou et al., 2016). Here we tested the methods using the mean and median parameters per PFT and climate type.

"PFT_{mean}": means for calibrated parameter vectors per PFT;
"$Clim_{mean}$": means for calibrated parameter vectors per main climate type;
"PFT_{med}": medians for calibrated parameter vectors per PFT;
"$Clim_{med}$": medians for calibrated parameter vectors per main climate type.

2.2.2. Similarity-Based Method ("$Site_{sim}$")

The site similarity is defined by Carvalhais et al. (2010) which measures the similarity (D) of the climate and vegetation features between site i and site j as in Equation 10:

$$D_{i,j} = 1 - \frac{\sum_{n=1}^{N} (\boldsymbol{V}_{i,n} - \boldsymbol{V}_{j,n})^2}{\sum_{n=1}^{N} \left(\boldsymbol{V}_{i,n} - \overline{\boldsymbol{V}_i}\right)^2} \tag{10}$$

Here, $\boldsymbol{V}_i$ is a vector including the normalized daily mean of the air temperature, precipitation (in logarithm), global radiation and LANDSAT-based normalized difference vegetation index (NDVI, see data source and processing method in Table S2 of the Supporting Information S1) between 1986 and 2015 at site i. N is the vector length ($=366 \times 4$) and $\overline{V_i}$ refers to the mean of $\boldsymbol{V}_i$.

To determine the parameters of a target location, we calculated D for each training site within the same PFT as the target location. The parameter vector at the site with the maximum D was used.

"$Site_{sim}$": parameter vectors for each site from the most similar site.

2.2.3. Optimization-Based Methods ("OPT-All" and "OPT-PFT")

The parameters can be optimized across all sites or at sites per PFT (Yuan et al., 2014a). Here we adopted the same algorithm, CMAES, and the same cost functions as the site-specific calibration method (see Text S1 in Supporting Information S1).

"OPT-All": a parameter vector optimized using all sites in the training data set (Yuan et al., 2014a).
"OPT-PFT": parameter vectors per PFT optimized using the sites within the same PFT in the training data set (Kuppel et al., 2012; Tian et al., 2020).

2.2.4. Regression-Based Methods ("sRF", "mRF", "mNN")

To test the assumption that calibrated parameters are determined by ecosystem properties, here we predict the calibrated parameters using the normalized features based on different regression methods.

"sRF": parameter vectors per site of which each parameter was predicted independently based on the single-output random forest (trees number = 100; Breiman, 2001).
"mRF": parameter vectors per site predicted simultaneously based on the multi-output random forest (trees number = 100; Pedregosa et al., 2011).
"mNN": parameter vectors per site predicted simultaneously based on the multi-layer perceptron neural network (hidden layers number = 2, neurons number = 16; Gardner & Dorling, 1998; McCulloch & Pitts, 1943).

2.2.5. Simultaneous Parameter Inversion and Extrapolation Based on Ecosystem Properties ("SPIE")

Models can suffer from equifinality problems, namely different parameter vectors can generate similar model performance. Consequently, the calibrated parameters may not represent the true parameters to simulate GPP,

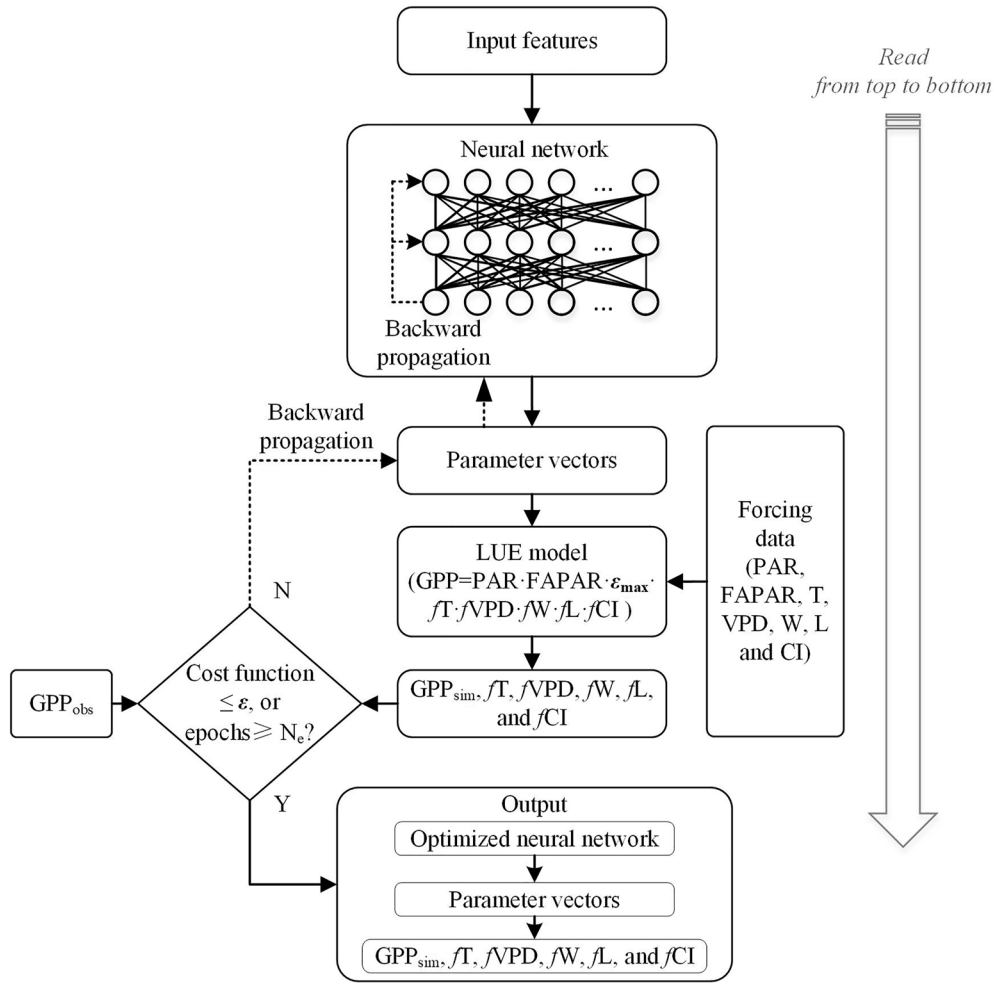

Figure 1. Flowchart of the SPIE approach. We rely on the learning of a neural network, that outputs parameter vectors per site, contingent on site-level input features (introduced in Section 2.1.2), and constrained by observation-based gross primary productivity fluxes and sensitivity functions (see the cost function definitions in Text S2 in Supporting Information S1). The training process stops once the tolerance value for the cost is passed ($\varepsilon = 10^{-2}$) or a maximum number of epochs are reached ($N_e = 2 \times 10^3$).

which reflect the GPP sensitivities controlled by the environmental properties. Here we additionally test the assumption that the predicted parameter vector based on ecosystem properties, which might differ from the calibrated parameter vector, can simulate GPP with good accuracy. Instead of directly predicting parameters constraining by calibrated or literature-referenced values, we applied the neural network to predict the parameters of a LUE model which is constrained by GPP_{obs}. The flowchart for this method is shown in Figure 1.

The sites were split into 10 groups according to the ten-fold cross-validation strategy to ensure robustness evaluation. Each training group includes all kinds of PFTs and climate types. For each group of training sites, the neural network takes the normalized site-level input features (Table S3 in Supporting Information S1) to predict simultaneously the individual site-level parameter vector (Table 1) for the LUE model to estimate GPP per site. GPP_{sim} is assessed against GPP_{obs} based on a custom cost function (see the equation of "cf_{NN}" in Text S2 of the Supporting Information S1). Further, parts of the cost function are the constraints of the sensitivity functions (see the equations of "cf_3" and "cf_4" in Text S1 of the Supporting Information S1). To optimize the neural network, we calculate the gradient of the cost function to each parameter and backpropagate the gradient to the weight and bias terms of each hidden layer with the gradient descent algorithm. Afterwards, the weight and bias of each neuron are optimized using the ADAM algorithm (Kingma & Ba, 2014). Either if the number of epochs reaches 2×10^3 or the cost function is below a defined threshold ($\varepsilon = 10^{-2}$), the optimization process stops. The hyperparameter of the neural network was tuned using a grid-searching approach (not shown here) which resulted in the following

values: learning rate = 10^{-3}, L_2 regularization coefficient = 10^{-4}, mini-batch size = 32, neurons per layer = 16 and hidden layers = 2. We apply the dropout strategy to the input and hidden layers, meaning that the neural network randomly deactivates a certain number of neurons in each batch. This leads to more robust predictions due to the avoidance of the overfitting problem (Srivastava et al., 2014). The output from the full pipeline is the trained neural network, which is then used to predict the parameter vector per site in test data sets. Finally, the LUE model with the predicted parameters is forced to simulate GPP and sensitivity functions (fT, fVPD, fW, fL, and fCI).

"SPIE": parameter vectors per site predicted based on ecosystem properties and constrained by both GPP errors and sensitivity functions of the LUE model.

2.2.6. Globally Fixed Method ("P-Model")

The P-model (B. D. Stocker et al., 2020; H. Wang et al., 2017) is derived based on Farquhar et al. (1980) and Fick's law together with an optimality theory (Prentice et al., 2014). All of its parameters are extracted from literature and upscaled from leaf-scale processes, therefore fixed globally. Mengoli et al. (2022) improved P-model from the original version by adding an acclimation process to the maximum rate of Rubisco activity and maximum rate of electron transport. Here we ran the Mengoli model based on daily data (introduced in Section 2.1.1). The P-model parameters were kept the same (acclimation window size = 15, running-mean approach based on daily data; Mengoli et al., 2022). The model outputs, GPP, were assessed against observations. The model performance was compared with the LUE model using other parameterization methods (Sections 2.2.1–2.2.5). It is emphasized here that P-model is different from the LUE model used in Sections 2.2.1–2.2.5 and that the acclimation process is only involved in the P-model.

"P-model": literature values which are applied globally.

2.3. Statistical Analysis for Parameterized Results

All the parameterization methods were assessed according to the GPP accuracy measured by Nash-Sutcliffe model efficiency (NSE, $(-\infty,1]$; NSE = 1 indicates a perfect model), determination coefficient (R^2, [0,1]; $R^2 = 1$ indicates a perfect model) and normalized root mean squared error (NRMSE, $[0,\infty)$; NRMSE = 0 indicates a perfect model) which is equal to the root mean squared error divided by the mean observational variable (e.g., GPP_{obs}). Only good-quality data were used to calculate NSE, R^2, and NRMSE. Here the good-quality data refers to the input vector of which the quality assessment flags (see "QA" and "QC" in Table S2 of the Supporting Information S1) are all higher than 0.8, including quality assessment flags of all meteorological inputs, vegetation index and GPP_{obs}. When aggregated to longer time scales, the good quality data means the average quality flags are all higher than 0.7 at the weekly and monthly scales, and 0.5 at the yearly scale. Besides, predicted parameters were compared to calibrated parameters to test if the model equifinality problem exists.

2.3.1. Site-Level Temporal GPP Assessment

We forced the LUE model at the daily scale and got the daily GPP_{sim} as a result. The weekly, monthly and yearly GPP_{sim} and GPP_{obs} were calculated based on the mean daily GPP_{sim} and GPP_{obs}, respectively. These time series of site-level GPP at different time scales were evaluated using NSE, R^2, and NRMSE. The vectors of NSE, R^2, and NRMSE were compared across all sites, per PFT and climate types.

2.3.2. Spatial Variability of GPP Assessment

The site-mean GPP_{obs} across sites represent the spatial variance of GPP. We used NSE, R^2, and NRMSE to measure the accuracy of the site-mean GPP_{sim} compared with GPP_{obs} to evaluate the ability of these parameterization methods to capture the spatial variability of GPP.

2.3.3. Comprehensive Assessment Across Spatio-Temporal Scales Based on Model Likelihood

The likelihood of each parameterization method, $\boldsymbol{P}$, was calculated according to Bao et al. (2022). To avoid selecting a method falling shortly at locally describing ecosystem GPP, $\boldsymbol{P}$ represents an overall performance at 200 different site groups. In each group, 100 sites were selected randomly from all sites and 2-year GPP was then randomly extracted from each of these 100 sites. The 200 site-years GPP_{sim} were compared to GPP_{obs} based on NSE, R^2, and NRMSE at each site-year independently. The differences between the daily, weekly, and monthly NSE, R^2, and NRMSE vectors and the yearly NRMSE vectors per parameterization method (each with 200

elements) were tested using Kolmogorov-Smirnov statistical test and *t*-test. The method with statistically higher NSE, R^2 or lower NRMSE than others was given with the largest score (=1, otherwise = 0) at each site group. In case that two or more methods were statistically equal and better than others, NSE, R^2, or NRMSE across all site-years was additionally computed to sort these methods independently. $\boldsymbol{P}$ is equal to the average score across all site groups. The average $\boldsymbol{P}$ across different statistical metrics (NSE, R^2, and NRMSE) and time scales (daily, weekly, monthly, and yearly) was used to detect the best parameterization method.

2.3.4. Comparison Between Predicted Parameters and Calibrated Parameters

Since the 13 parameters have different meanings and ranges, they were compared independently. The similarity between the predicted parameters using methods introduced in Section 2.2 and the calibrated parameters based on the observational data (see Text S1 in Supporting Information S1) was assessed using NSE, R^2, and NRMSE.

2.4. Feature Importance Estimation

We evaluated the importance of input features using three methods and selected the most important features based on the average normalized feature importance values.

2.4.1. Shapley-Based Feature Importance (SHAP)

The Shapley value of a feature is calculated based on the deviation of the predicted parameter at a certain input from the average prediction (Lundberg & Lee, 2017), which represents the contribution of a feature to the output. Here SHAP is equal to the average absolute Shapley value across all inputs. The average SHAP across all cross-validation groups (Friedman, 2001) was used to assess the contribution of features for each parameter and all parameters.

2.4.2. Layer-Wise-Relevance-Propagation-Based Feature Importance (LRP)

The layer-wise relevance propagation refers to a strategy that allows decomposing the prediction of the neural network over an input feature (Montavon et al., 2019). It is usually used in deep classification neural networks, here we applied LRP to assess a shallow regression neural network. We calculated the relevance vector according to Bach et al. (2015) and measured the feature importance according to the average relevance across different cross-validation groups.

2.4.3. Partial-Dependence-Based Feature Importance (PD)

We estimated the partial dependence of the prediction on each input feature based on Friedman's (2001) algorithm. The feature importance, PD, was measured according to the partial dependence, which is equal to the standard deviation of the partial dependence if the input feature is non-categorical variables, otherwise is equal to the one-fourth of the absolute partial dependence range (Greenwell et al., 2018).

3. Results

3.1. Temporal and Spatial Assessment

The parameterization method based on the neural network aiming at minimizing GPP errors and constraining sensitivity functions, SPIE, had the best performance compared with other typical parameterization methods. All the assessing metrics at daily, weekly, monthly, and yearly scales, NSE (Figure 2), R^2 (Figure S1 in Supporting Information S1) and NRMSE (Figure S2 in Supporting Information S1), showed that SPIE was better at more sites (i.e., more bright color blocks in Figure 2). The spatial variability of GPP can be also better captured by SPIE, which had higher NSE, R^2, and lower NRMSE measured by site-mean GPP_{obs} and GPP_{sim} (Figure 3). The accuracy of time series and site-mean GPP_{sim} using other methods were all significantly worse than SPIE. The results of these parameterization methods were also compared to those of site-specific calibrations ("site-calib", see details in Section 2.1.1). In the following analyses, the performance of "site-calib" is set as the benchmark of the cross-validation exercises since it represents the maximum NSE would reach in any of the out-of-sample prediction approaches. Although SPIE cannot perform as well as the site-specific calibration, it is the best parameter extrapolation method globally.

The global best parameterization method, SPIE, outperformed across various PFTs and climate types. It had the highest daily NSE quantiles for each PFT and climate type considered in this study (Figure 4). While SPIE was

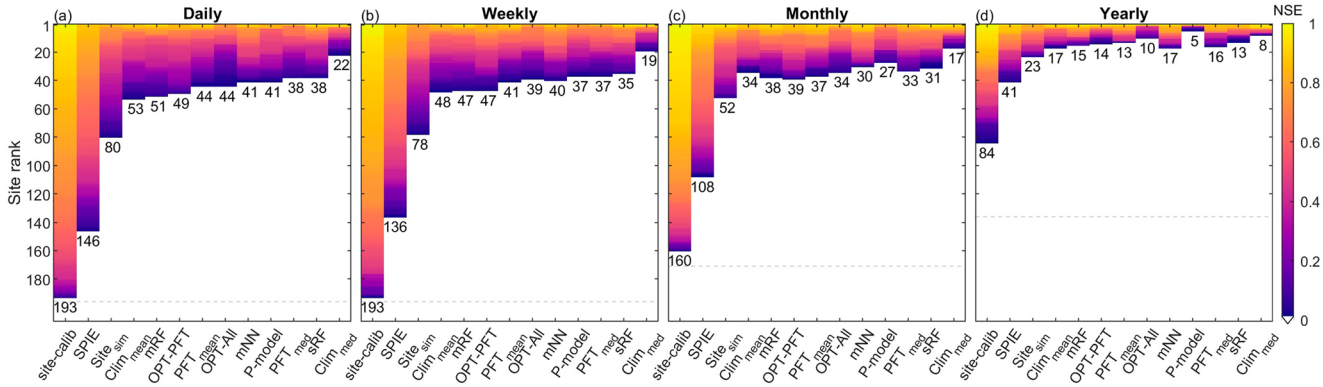

Figure 2. Comparison of NSE between GPP_{obs} and GPP_{sim} based on 12 different parameterization methods (see definitions of PFT_{mean}, $Clim_{mean}$, PFT_{med}, $Clim_{med}$, $Site_{sim}$, OPT-All, OPT-PFT, sRF, mRF, mNN, SPIE, and P-model in Section 2.2), and NSE between GPP_{obs} and GPP_{calib} ("site-calib", see the calibration process in Text S1 of the Supporting Information S1) at daily (a), weekly (b), monthly (c) and yearly (d) scales. The methods are sorted according to the number of sites with positive NSE, which is displayed under each bar. The sites with negative NSE are in white color. The area under the gray dashed line represents the sites excluded in the comparison due to less than four good-quality (see the definition of "good-quality" data in Section 2.3) data points.

relatively better than other methods, no extrapolated parameters can provide accurate GPP dynamics (NSE > 0.4) at closed shrubland (Figure 4c), woody savanna (Figure 4l), tropical (Figure 4m) and polar (Figure 4q) climate types given that the model using calibrated parameters was good. It demonstrated that the variance of current extrapolated parameters was still insufficient and the parameters are possible to be overfitted in site calibrations. Using R^2 or NRMSE as the assessing metric (see details in Figures S3 and S4 of the Supporting Information S1), the parameterization methods showed smaller but robust relative differences, that is, the SPIE was still the best method. In general, while none of these parameter extrapolation methods can reach the highest model performance, SPIE was the best option for areas without observational data.

The model likelihood, ***P***, which represents the likelihood of a model statistically better than others across various site groups, illustrated that SPIE was the best method to extrapolate parameters, followed by OPT-All and $Clim_{med}$ with likelihoods lower than 0.06 (i.e., at less than 6% groups of sites the two methods can outperform). The average ***P*** of SPIE across daily, weekly, monthly, and yearly scales, and across various assessing metrics was also significantly higher than the other methods. It represented that the method is robust across multiple temporal and spatial scales.

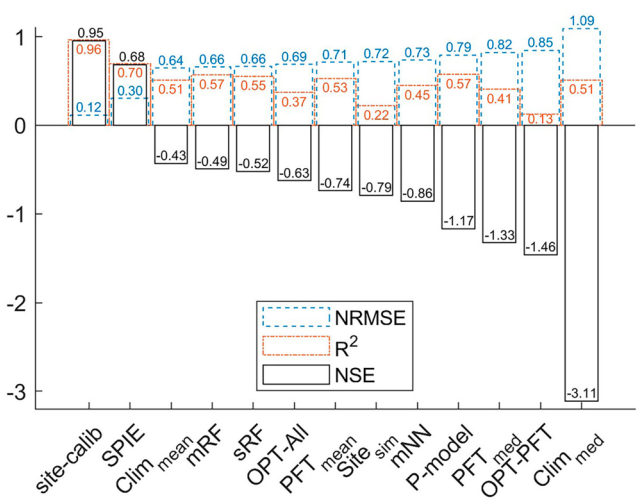

Figure 3. Comparison of NSE, R^2, and normalized root mean squared error between the site-mean GPP_{obs} and GPP_{sim}. The bars (i.e., parameterization methods) are sorted according to NSE.

3.2. Differences Between Calibrated Parameters and Predicted Parameters

The predicted parameters displayed different distribution patterns from the calibrated parameters. Taking the best method, SPIE, as an example (Figure 6), ranges of predicted parameters were narrower than calibrated parameters given the same predefined range. Further, SPIE predicted parameters had no "edge-hitting" problem, which means that the parameter frequently reaches its maximum or minimum values, for example, the calibrated parameters T_{opt}, k_T, C_κ, C_{a0}, C_m and k_W (gray bars in Figures 6b–6c, 6f–6h, and 6j). The other parameterization methods based on ecosystem properties (e.g., mRF, Figure S5 in Supporting Information S1) also showed narrower ranges. However, clustering and optimization-based methods had similar ranges to the site-specific calibrations and more edge-hitting instances than SPIE (see details in Figures S6 and S7 of the Supporting Information S1).

The LUE model performance was not determined by the parameter difference to site-specific calibrations. For example, NSE between the predicted parameters using SPIE and calibrated parameters across sites were all negative. The maximum R^2 was 0.08 and the lowest NRMSE was 0.08. Furthermore, the NSE difference between the calibration and SPIE was not correlated with

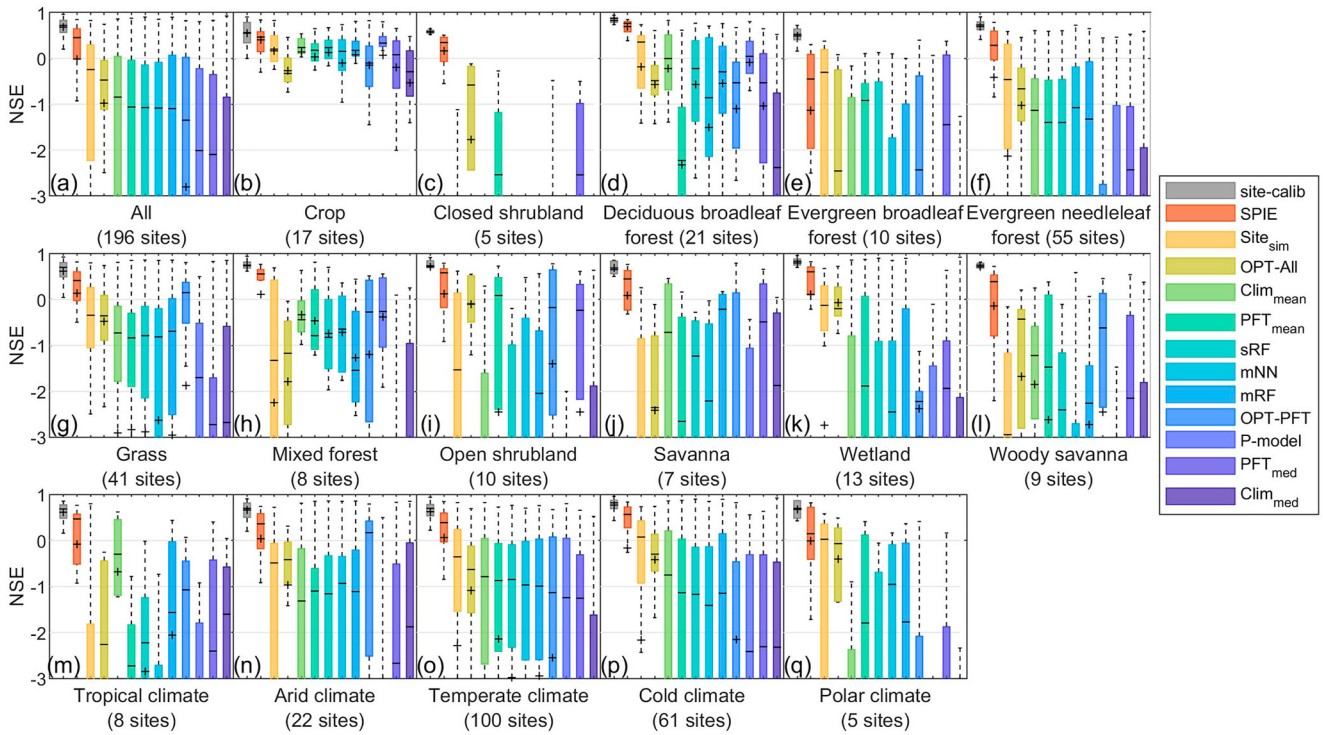

Figure 4. Site-level daily NSE comparison across all sites (a), per plant functional type (b–l) and climate type (m–q). The mean and median per type are represented by the black cross and the black line, respectively. The methods are sorted according to NSE medians across all sites. The area where NSE is lower than minus three is not displayed.

the relative difference between calibrated and predicted parameters (Figure 7). Thus, the predicted parameters were not comparable to the calibrated parameters while they can produce similar GPP, suggesting the overfitting and parameter equifinality in the site-specific calibrations of LUE model. It also reflects the potential risk in applying calibrated parameters as the ground truth to make predictions or extrapolations of model parameters in space.

3.3. Important Features for Explaining Model Parameter Variability

The average normalized values of SHAP, LRP and PD illustrated that bioclimatic variables, soil properties, and VIF were the most important feature classes explaining the spatial variability of model parameters (Figure 8). The importance values differed across three different methods, but all of them showed that atmospheric NPdep was not an important feature class. However, the original SHAP shows that atmospheric phosphorus deposition was the tenth important feature (Figure S8b in Supporting Information S1). Some specific PFTs, for example, DBF and MF, had relatively higher SHAP and LRP (Figures S8b and S8c in Supporting Information S1), indicating that their relative parameter vectors had different ranges compared to other PFTs. All approaches showed that most climate types were not important for determining model parameters (see details in Figures S8a–S8d of the Supporting Information S1). Given the divergence among approaches, the specific important feature was hard to determine. The approach differences also existed in each parameter, while the ranks of feature classes remained in the same order as the ranks for all parameters (Figure S9 in Supporting Information S1). On average, the most important feature classes were bioclimatic variables, soil properties, and VIF.

4. Discussion

4.1. Well-Constrained Site-Specific Parameterization Is Better Than PFT-Dependent Parameterization

It has been shown that the long-used PFT-based parameterization cannot capture the variance in parameters within PFT (Bloom et al., 2016) and can be influenced by PFT misclassification errors. The method of directly using parameters from papers without local or global evaluation can be also risky. P-model which adopted the

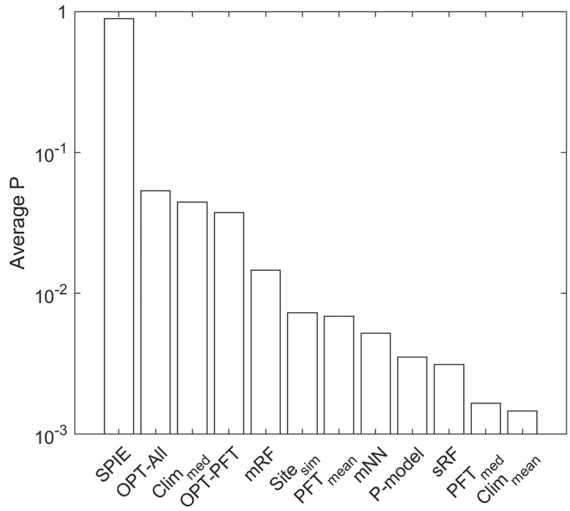

Figure 5. The average model likelihood (*P*) of parameterization methods.

globally fixed parameters upscaled from the leaf scale might not include PFT errors (Mengoli et al., 2022; B. D. Stocker et al., 2020), but had limited accuracy across temporal (Figure 2) and spatial scales (Figure 3). Here, results showed that the globally fixed parameterization method (e.g., P-model) was worse than the PFT-based method (e.g., OPT-PFT, and PFT_{mean}). The global optimization method (e.g., OPT-All) had slightly better performance than PFT-based optimization at the global scale (Figure 5) due to higher spatial generalizability (e.g., Figure 3), the same as Yuan et al. (2014a). However, OPT-All had accurate predictions at fewer sites (Figure 2). This agrees with a study using the PRELES model (Tian et al., 2020), which demonstrated that globally optimized parameters are not sufficient to reflect the variability of GPP sensitivities. Luo and Schuur (2020) also confirmed that model parameters should vary with the spatial and temporal changes of ecosystem properties but not depend on PFTs. While the site-specific parameterizations ($Site_{sim}$, sRF, mRF, and mNN) have higher flexibility than clustering methods (PFT_{mean}, $Clim_{mean}$, PFT_{med}, and $Clim_{med}$), they did not show a robust advantage due to uncertainties remained in the calibrated parameters, which were used to constrain the predicted parameters in these methods. However, the site-specific parameterization constraining GPP prediction errors and sensitivity functions, SPIE, reaches the highest performance, highlighting that the well-constrained site-specific parameterization method can provide more reliable outputs than clustering and optimization methods. This is the opposite of the conclusion of Tian et al. (2020) who tested only the site-specific optimization method showing higher uncertainties than the PFT-based optimization method.

4.2. Reduced Parameter Variability by Considering the Relationship Between Parameters and Ecosystem Properties

Our results reveal the equifinality of model parameters, which consequently increases the model uncertainty. While no extrapolated parameter vectors outperformed calibrated ones, parameter ranges were better constrained in all methods based on ecosystem properties (e.g., sRF, mRF, mNN, and SPIE) compared with site calibrations, clustering and optimization methods. The results of parameter distribution and GPP simulation performance demonstrate that considering physical links between GPP sensitivities and ecosystem properties can reduce the parameter equifinality and the overfitting in site-specific calibrations. This is also true in other LUE models (Horn & Schulz, 2011b). Furthermore, SPIE, considering only the GPP errors and constraints on sensitivity functions but not the distance to calibrated parameters, avoids inheriting uncertainties from model calibration. In general, the model parameterization relying on ecosystem properties can reduce the parameter uncertainty resulting from model equifinality.

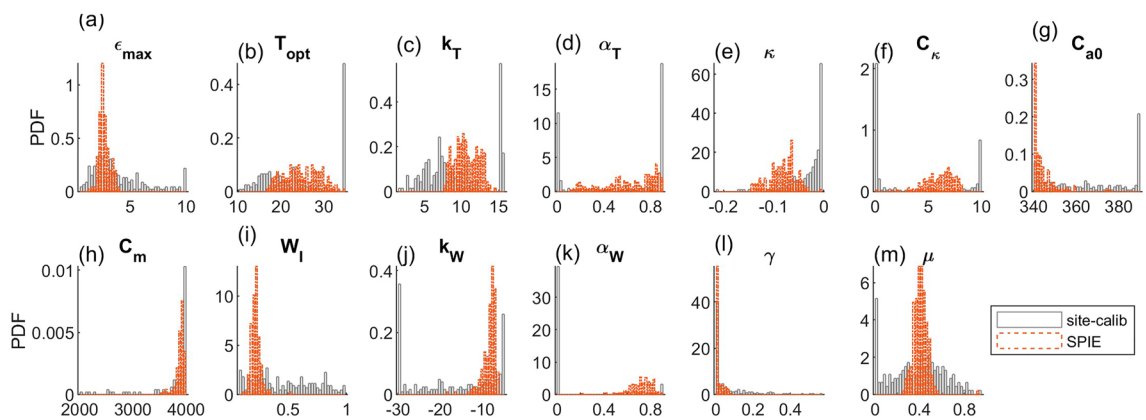

Figure 6. Probability density function of the calibrated parameters (site-calib) and the predicted parameters by SPIE.

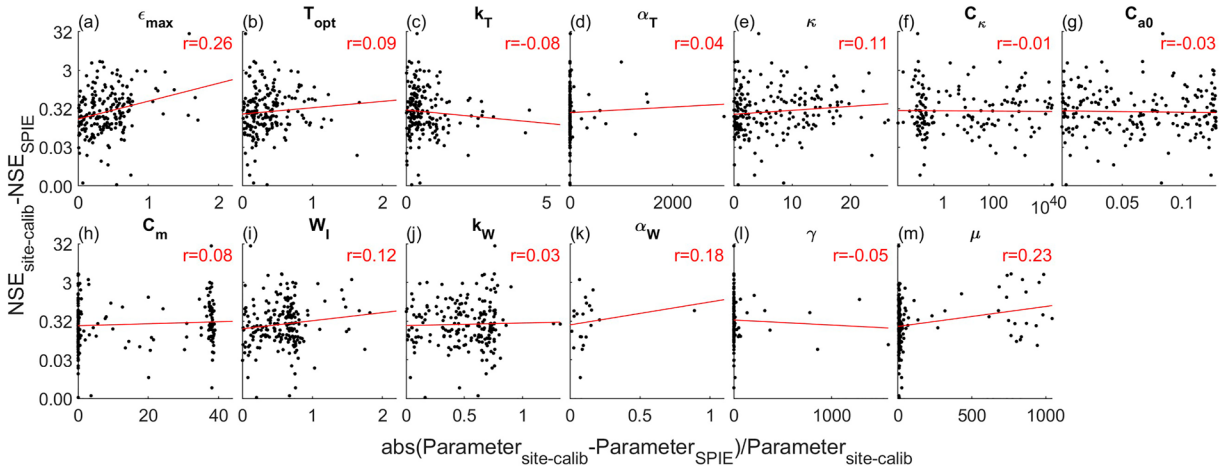

Figure 7. The distribution of site-level NSE differences between site-specific calibration ($NSE_{site-calib}$) and SPIE (NSE_{SPIE}) with the relative differences between calibrated parameters and predicted parameters. The red line is the least-squares fitting line of the scatters. The correlation coefficient (r) is displayed at the upper-right corner.

4.3. Drivers of the Spatial Variability of GPP Sensitivities

Overall, the information in bioclimatic variables, soil properties and vegetation features explain most of the spatial variation in predicted parameters by SPIE (Figure 8). Taking $\mathbf{T_{opt}}$ as an example, our results display that this parameter is controlled by bioclimatic variables primarily (Figure S9b in Supporting Information S1), followed by soil properties and vegetation features. PFT is the fourth important feature determining the spatial variability of $\mathbf{T_{opt}}$. The results agree partly with Huang et al. (2019) and Chang et al. (2020), which illustrate the relationship of $\mathbf{T_{opt}}$ to mean annual temperature and vegetation index, respectively. These two studies together with ours showed that bioclimatic variables, soil properties and vegetation features cannot be neglected in determining $\mathbf{T_{opt}}$. Furthermore, bioclimatic variables, vegetation features and soil properties presented higher importance than PFT for other parameters of the LUE model. The parameters varying with six classes of features are significantly better than those parameters only varying with PFT or without spatial variability (Figures 2–5). The results are in contrast to studies supporting PFT-based and globally fixed parameterization (Tian et al., 2020; Yuan et al., 2014a). However, the general observation is similar to the results of other independent studies using a different LUE model (Horn & Schulz, 2011b) and terrestrial biosphere models (Peaucelle et al., 2019). These two studies also demonstrated that ecosystem model parameters are controlled by climate and vegetation features along with PFT. Our study highlights the significance of considering more ecosystem properties including vegetation features, climate conditions and soil properties in ecosystem model parameterization. Given our assumption that model parameters indicate ecosystem sensitivities, the results demonstrate the ecological understanding that vegetation features, climate conditions, soil properties along with plant forms impose instrumental controls on how ecosystems respond to environmental changes.

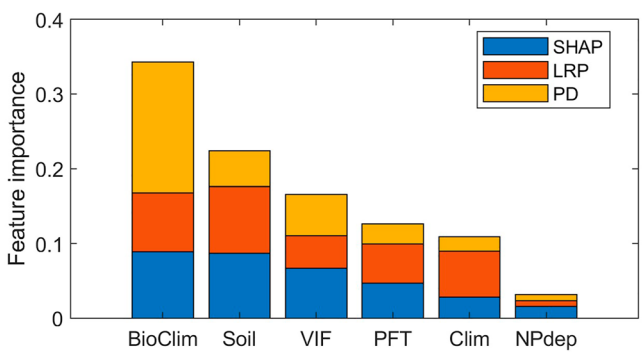

Figure 8. The input feature classes sorted by the average normalized SHAP, LRP, and PD for all parameters. The original SHAP, LRP, and PD were divided by the sum to get the normalized values. The sum of all bars is equal to one. The detailed average SHAP, LRP, and PD values per feature are displayed in Figure S8 of the Supporting Information S1. The feature classes (see definitions in Table S3 of the Supporting Information S1) refer to plant functional types, Koeppen-Geiger climate classification types (Clim), bioclimatic variables and aridity indexes (BioClim), vegetation index features, atmospheric nitrogen and phosphorus deposition and soil properties (Soil).

However, the current approach needs further development toward pinpointing key features controlling the spatial variability of parameters. On the one hand, strong covariation between input features (Figure S10 in Supporting Information S1) limits a confident variable attribution. On the other hand, differences in variable importance between different methods (e.g., SHAP, LRP, and PD) may result in different variable rankings (Figures S8 and S9 in Supporting Information S1). These may be associated with the covariation between features as well as the underlying assumptions per feature importance estimation method. However, given stationarity in the correlation structure between features, none of these aspects would limit a statistical extrapolation of parameter variability in space.

Differences in the model fitness between the site calibration and SPIE may reflect common overfitting issues in standard calibration exercises, challenging the generalization of a given GPP model and/or of features and architectures for the extrapolation approach. Exploring the contribution of additional variables may be a model-specific exercise, for example, illumination features, as in the model of Horn and Schulz (2011b), that can contribute to the enhanced spatial variance in predicted parameters.

Given the background understanding that ecosystem properties, including vegetation features, climate regimes, soil characteristics and other environmental traits, influence response sensitivities of carbon assimilation fluxes to environmental conditions, our results suggest further expanding SPIE approach to other kinds of terrestrial ecosystem carbon cycle models (e.g., land surface models and dynamic global vegetation models). Yet, temporal changes in ecosystem properties can affect parameters (Luo & Schuur, 2020). Our results also suggest a cautionary remark regarding the temporal variation in parameters when extrapolating or applying parameters to long time scales (e.g., beyond decadal scales in prognostic simulations).

5. Conclusions

In this study, we developed a model parameterization approach based on the link between ecosystem sensitivities and properties constrained by GPP simulation errors and sensitivity functions. The method leverages a neural network method to learn the parameterization of an LUE model. Moreover, the experimental design demonstrates that the method enables parameter extrapolation in regions without observational data with significantly and substantially higher accuracy than the widely used PFT-based and globally fixed parameterization methods. Compared with a set of univariate clustering, similarity-, regression-based and fixed methods (NSE > 0 at less than 41% of sites) considered in this study, our approach uniquely predicts GPP fluxes with confidence in cross-validation (NSE > 0 at 74% of sites). The resulting reduction in parameter variability through prediction via ecosystem properties suggests reductions in equifinality and overfitting, which commonly emerge from site-specific parameterizations. Vegetation features, bioclimatic variables, soil properties and some PFTs can explain the spatial variability of LUE model parameters. Overall, these are key features for diagnostic modeling exercises, although the temporal variation in the parameters and the relationship between them and ecosystem properties need further exploration toward prognostic modeling. Given the general need for biological and ecological parameterizations in carbon and water terrestrial ecosystem models, our results propose statistical learning approaches for the parameterization of land surface schemes in Earth system models.

Data Availability Statement

Meteorological input data for the LUE model is available at the website of FLUXNET (Pastorello et al., 2020). The FluxnetEO product used for extracting vegetation index is accessed from ICOS Carbon Portal for LANDSAT (Walther et al., 2022a) and for MODIS (Walther et al., 2022b). CRUNCEP data set for calculating bioclimatic variables is available at NCAR (Viovy, 2018). Atmospheric NPdep data (R. Wang et al., 2017) are extracted and applied as elements of input features. SoilGrids product is accessed through WCS tool (Poggio et al., 2021). The neural network framework was developed using trainNetwork (Kudo et al., 1999) introduced in MATLAB 2022a, available under MATLAB license at https://www.mathworks.com/products/matlab.html. Data were processed and figures were made with MATLAB 2022a. The model outputs, parameters and scripts supporting the analysis and production of figures are available at Bao and Carvalhais (2023).

Acknowledgments
This work has received funding from the European Union's Horizon 2020 Research and Innovation Project DeepCube "Explainable AI pipelines for big Copernicus data" (Grant agreement No. 101004188), from the Youth Innovation Subject 2022 of National Space Science Center, Chinese Academy of Sciences, Sino-German (CSC-DAAD) Postdoc Scholarship Program, and from the European Space Agency (ESA) via the Earth System Data Lab (ESDL). This work used eddy covariance data acquired and shared by the FLUXNET community, including these networks: AmeriFlux, AfriFlux, AsiaFlux, CarboAfrica, CarboEuropeIP, CarboItaly, CarboMont, ChinaFlux, Fluxnet-Canada, GreenGrass, ICOS, KoFlux, LBA, NECC, OzFlux-TERN, TCOS-Siberia, and USCCC. The FLUXNET eddy covariance data processing and harmonization was carried out by the ICOS Ecosystem Thematic Center, AmeriFlux Management Project and Fluxdata project of FLUXNET, with the support of CDIAC, and the OzFlux, ChinaFlux and AsiaFlux offices.

References

Bach, S., Binder, A., Montavon, G., Klauschen, F., Müller, K.-R., & Samek, W. (2015). On pixel-wise explanations for non-linear classifier decisions by layer-wise relevance propagation. *PLoS One*, *10*(7), e0130140. https://doi.org/10.1371/journal.pone.0130140

Baldocchi, D., Ryu, Y., & Keenan, T. (2016). Terrestrial carbon cycle variability. *F1000Research*, *5*, 5. https://doi.org/10.12688/f1000research.8962.1

Bao, S., & Carvalhais, N. (2023). Dataset and scripts for ToRobustParInPhotosynthesismodels [Dataset]. Zenodo. https://doi.org/10.5281/zenodo.7771525

Bao, S., Wutzler, T., Koirala, S., Cuntz, M., Ibrom, A., Besnard, S., et al. (2022). Environment-sensitivity functions for gross primary productivity in light use efficiency models. *Agricultural and Forest Meteorology*, *312*, 108708. https://doi.org/10.1016/j.agrformet.2021.108708

Bloom, A. A., & Williams, M. (2015). Constraining ecosystem carbon dynamics in a data-limited world: Integrating ecological "common sense" in a model–data fusion framework. *Biogeosciences*, *12*(5), 1299–1315. https://doi.org/10.5194/bg-12-1299-2015

Bloom, A. A., Exbrayat, J.-F., Van Der Velde, I. R., Feng, L., & Williams, M. (2016). The decadal state of the terrestrial carbon cycle: Global retrievals of terrestrial carbon allocation, pools, and residence times. *Proceedings of the National Academy of Sciences of the United States of America*, *113*(5), 1285–1290. https://doi.org/10.1073/pnas.1515160113

Breiman, L. (2001). Random forests. *Machine Learning*, *45*(1), 5–32. https://doi.org/10.1023/a:1010933404324

Carvalhais, N., Reichstein, M., Collatz, G., Mahecha, M., Migliavacca, M., Neigh, C., et al. (2010). Deciphering the components of regional net ecosystem fluxes following a bottom-up approach for the Iberian Peninsula. *Biogeosciences*, *7*(11), 3707–3729. https://doi.org/10.5194/bg-7-3707-2010

Carvalhais, N., Reichstein, M., Seixas, J., Collatz, G. J., Pereira, J. S., Berbigier, P., et al. (2008). Implications of the carbon cycle steady state assumption for biogeochemical modeling performance and inverse parameter retrieval. *Global Biogeochemical Cycles*, *22*(2). https://doi.org/10.1029/2007gb003033

Chang, Q., Xiao, X., Wu, X., Doughty, R., Jiao, W., Bajgain, R., et al. (2020). Estimating site-specific optimum air temperature and assessing its effect on the photosynthesis of grasslands in mid- to high-latitudes. *Environmental Research Letters*, *15*(3), 034064. https://doi.org/10.1088/1748-9326/ab70bb

Ciais, P., Tan, J., Wang, X., Roedenbeck, C., Chevallier, F., Piao, S.-L., et al. (2019). Five decades of northern land carbon uptake revealed by the interhemispheric CO_2 gradient. *Nature*, *568*(7751), 221–225. https://doi.org/10.1038/s41586-019-1078-6

Farquhar, G. D., von Caemmerer, S. V., & Berry, J. A. (1980). A biochemical model of photosynthetic CO_2 assimilation in leaves of C3 species. *Planta*, *149*(1), 78–90. https://doi.org/10.1007/bf00386231

Frankenberg, C., Fisher, J. B., Worden, J., Badgley, G., Saatchi, S. S., Lee, J. E., et al. (2011). New global observations of the terrestrial carbon cycle from GOSAT: Patterns of plant fluorescence with gross primary productivity. *Geophysical Research Letters*, *38*(17), L17706. https://doi.org/10.1029/2011gl048738

Friedman, J. H. (2001). Greedy function approximation: A gradient boosting machine. *Annals of Statistics*, *29*(5), 1189–1232. https://doi.org/10.1214/aos/1013203451

Gardner, M. W., & Dorling, S. (1998). Artificial neural networks (the multilayer perceptron)—A review of applications in the atmospheric sciences. *Atmospheric environment*, *32*(14–15), 2627–2636. https://doi.org/10.1016/s1352-2310(97)00447-0

Greenwell, B. M., Boehmke, B. C., & McCarthy, A. J. (2018). A simple and effective model-based variable importance measure. *arXiv preprint arXiv:1805.04755*.

Groenendijk, M., Dolman, A., Van der Molen, M., Leuning, R., Arneth, A., Delpierre, N., et al. (2011). Assessing parameter variability in a photosynthesis model within and between plant functional types using global Fluxnet eddy covariance data. *Agricultural and Forest Meteorology*, *151*(1), 22–38. https://doi.org/10.1016/j.agrformet.2010.08.013

Guan, X., Chen, J. M., Shen, H., Xie, X., & Tan, J. (2022). Comparison of big-leaf and two-leaf light use efficiency models for GPP simulation after considering a radiation scalar. *Agricultural and Forest Meteorology*, *313*, 108761. https://doi.org/10.1016/j.agrformet.2021.108761

Hansen, N., & Kern, S. (2004). Evaluating the CMA evolution strategy on multimodal test functions. In *Paper presented at the international conference on parallel problem solving from nature*.

He, M., Ju, W., Zhou, Y., Chen, J., He, H., Wang, S., et al. (2013). Development of a two-leaf light use efficiency model for improving the calculation of terrestrial gross primary productivity. *Agricultural and Forest Meteorology*, *173*, 28–39. https://doi.org/10.1016/j.agrformet.2013.01.003

Horn, J., & Schulz, K. (2011a). Identification of a general light use efficiency model for gross primary production. *Biogeosciences*, *8*(4), 999–1021. https://doi.org/10.5194/bg-8-999-2011

Horn, J., & Schulz, K. (2011b). Spatial extrapolation of light use efficiency model parameters to predict gross primary production. *Journal of Advances in Modeling Earth Systems*, *3*(4). https://doi.org/10.1029/2011ms000070

Huang, M., Piao, S., Ciais, P., Peñuelas, J., Wang, X., Keenan, T. F., et al. (2019). Air temperature optima of vegetation productivity across global biomes. *Nature Ecology & Evolution*, *3*(5), 772–779. https://doi.org/10.1038/s41559-019-0838-x

Huntzinger, D. N., Michalak, A. M., Schwalm, C., Ciais, P., King, A. W., Fang, Y., et al. (2017). Uncertainty in the response of terrestrial carbon sink to environmental drivers undermines carbon-climate feedback predictions. *Scientific Reports*, *7*(1), 4765. https://doi.org/10.1038/s41598-017-03818-2

Jung, M., Reichstein, M., Margolis, H. A., Cescatti, A., Richardson, A. D., Arain, M. A., et al. (2011). Global patterns of land-atmosphere fluxes of carbon dioxide, latent heat, and sensible heat derived from eddy covariance, satellite, and meteorological observations. *Journal of Geophysical Research*, *116*(G3), G00J07. https://doi.org/10.1029/2010jg001566

Kalliokoski, T., Makela, A., Fronzek, S., Minunno, F., & Peltoniemi, M. (2018). Decomposing sources of uncertainty in climate change projections of boreal forest primary production. *Agricultural and Forest Meteorology*, *262*, 192–205. https://doi.org/10.1016/j.agrformet.2018.06.030

Kingma, D. P., & Ba, J. (2014). Adam: A method for stochastic optimization. *arXiv preprint arXiv:1412.6980*.

Kudo, M., Toyama, J., & Shimbo, M. (1999). Multidimensional curve classification using passing-through regions. *Pattern Recognition Letters*, *20*(11–13), 1103–1111. https://doi.org/10.1016/s0167-8655(99)00077-x

Kuppel, S., Peylin, P., Chevallier, F., Bacour, C., Maignan, F., & Richardson, A. (2012). Constraining a global ecosystem model with multi-site eddy-covariance data. *Biogeosciences*, *9*(10), 3757–3776. https://doi.org/10.5194/bg-9-3757-2012

Lundberg, S. M., & Lee, S.-I. (2017). A unified approach to interpreting model predictions. In *Paper presented at the 31st annual conference on neural information processing systems (NIPS)*.

Luo, Y., & Schuur, E. A. G. (2020). Model parameterization to represent processes at unresolved scales and changing properties of evolving systems. *Global Change Biology*, *26*(3), 1109–1117. https://doi.org/10.1111/gcb.14939

Mahadevan, P., Wofsy, S. C., Matross, D. M., Xiao, X., Dunn, A. L., Lin, J. C., et al. (2008). A satellite-based biosphere parameterization for net ecosystem CO_2 exchange: Vegetation Photosynthesis and Respiration Model (VPRM). *Global Biogeochemical Cycles*, *22*(2). https://doi.org/10.1029/2006gb002735

Mäkelä, A., Pulkkinen, M., Kolari, P., Lagergren, F., Berbigier, P., Lindroth, A., et al. (2008). Developing an empirical model of stand GPP with the LUE approach: Analysis of eddy covariance data at five contrasting conifer sites in Europe. *Global Change Biology*, *14*(1), 92–108. https://doi.org/10.1111/j.1365-2486.2007.01463.x

Masson-Delmotte, V., Zhai, P., Pirani, A., Connors, S. L., Péan, C., Berger, S., et al. (2021). Climate change 2021: The physical science basis. In *Contribution of working group I to the sixth assessment report of the intergovernmental panel on climate change* (Vol. 2).

McCulloch, W. S., & Pitts, W. (1943). A logical calculus of the ideas immanent in nervous activity. *Bulletin of Mathematical Biophysics*, *5*(4), 115–133. https://doi.org/10.1007/bf02478259

Medlyn, B. E., Robinson, A. P., Clement, R., & McMurtrie, R. E. (2005). On the validation of models of forest CO_2 exchange using eddy covariance data: Some perils and pitfalls. *Tree Physiology*, *25*(7), 839–857. https://doi.org/10.1093/treephys/25.7.839

Mengoli, G., Agusti-Panareda, A., Boussetta, S., Harrison, S. P., Trotta, C., & Prentice, I. C. (2022). Ecosystem photosynthesis in land-surface models: A first-principles approach incorporating acclimation. *Journal of Advances in Modeling Earth Systems*, *14*(1). https://doi.org/10.1029/2021ms002767

Montavon, G., Binder, A., Lapuschkin, S., Samek, W., & Müller, K.-R. (2019). Layer-wise relevance propagation: An overview. *Explainable AI: Interpreting, Explaining and Visualizing Deep Learning*, 193–209. https://doi.org/10.1007/978-3-030-28954-6_10

Monteith, J. (1972). Solar radiation and productivity in tropical ecosystems. *Journal of Applied Ecology*, *9*(3), 747–766. https://doi.org/10.2307/2401901

Pastorello, G., Trotta, C., Canfora, E., Chu, H., Christianson, D., Cheah, Y.-W., et al. (2020). The FLUXNET2015 dataset and the ONEFlux processing pipeline for eddy covariance data [Dataset]. FLUXNET, *7*, 225. https://fluxnet.org/

Peaucelle, M., Bacour, C., Ciais, P., Vuichard, N., Kuppel, S., Peñuelas, J., et al. (2019). Covariations between plant functional traits emerge from constraining parameterization of a terrestrial biosphere model. *Global Ecology and Biogeography*, *28*(9), 1351–1365. https://doi.org/10.1111/geb.12937

Pedregosa, F., Varoquaux, G., Gramfort, A., Michel, V., Thirion, B., Grisel, O., et al. (2011). Scikit-learn: Machine learning in Python. *Journal of Machine Learning Research*, *12*, 2825–2830.

Piao, S., Wang, X., Wang, K., Li, X., Bastos, A., Canadell, J. G., et al. (2020). Interannual variation of terrestrial carbon cycle: Issues and perspectives. *Global Change Biology*, *26*(1), 300–318. https://doi.org/10.1111/gcb.14884

Poggio, L., de Sousa, L. M., Batjes, N. H., Heuvelink, G. B. M., Kempen, B., Ribeiro, E., & Rossiter, D. (2021). SoilGrids 2.0: Producing soil information for the globe with quantified spatial uncertainty [Dataset]. SoilGrids, *7*, 217–240. https://doi.org/10.5194/soil-7-217-2021

Potter, C. S., Randerson, J. T., Field, C. B., Matson, P. A., Vitousek, P. M., Mooney, H. A., & Klooster, S. A. (1993). Terrestrial ecosystem production: A process model based on global satellite and surface data. *Global Biogeochemical Cycles*, *7*(4), 811–841. https://doi.org/10.1029/93gb02725

Prentice, I. C., Dong, N., Gleason, S. M., Maire, V., & Wright, I. J. (2014). Balancing the costs of carbon gain and water transport: Testing a new theoretical framework for plant functional ecology. *Ecology Letters*, *17*(1), 82–91. https://doi.org/10.1111/ele.12211

Rubel, F., Brugger, K., Haslinger, K., & Auer, I. (2017). The climate of the European Alps: Shift of very high resolution Köppen-Geiger climate zones 1800–2100. *Meteorologische Zeitschrift*, *26*(2), 115–125. https://doi.org/10.1127/metz/2016/0816

Running, S. W., Nemani, R. R., Heinsch, F. A., Zhao, M., Reeves, M., & Hashimoto, H. (2004). A continuous satellite-derived measure of global terrestrial primary production. *BioScience*, *54*(6), 547–560. https://doi.org/10.1641/0006-3568(2004)054[0547:acsmog]2.0.co;2

Ryu, Y., Berry, J. A., & Baldocchi, D. D. (2019). What is global photosynthesis? History, uncertainties and opportunities. *Remote Sensing of Environment*, *223*, 95–114. https://doi.org/10.1016/j.rse.2019.01.016

Srivastava, N., Hinton, G., Krizhevsky, A., Sutskever, I., & Salakhutdinov, R. (2014). Dropout: A simple way to prevent neural networks from overfitting. *Journal of Machine Learning Research*, *15*, 1929–1958.

Stocker, B. D., Wang, H., Smith, N. G., Harrison, S. P., Keenan, T. F., Sandoval, D., et al. (2020). P-model v1. 0: An optimality-based light use efficiency model for simulating ecosystem gross primary production. *Geoscientific Model Development*, *13*(3), 1545–1581. https://doi.org/10.5194/gmd-13-1545-2020

Stocker, T. (2014). *Climate change 2013: The physical science basis: Working group I contribution to the fifth assessment report of the intergovernmental panel on climate change*. Cambridge University Press.

Tian, X., Minunno, F., Cao, T., Peltoniemi, M., Kalliokoski, T., & Mäkelä, A. (2020). Extending the range of applicability of the semi-empirical ecosystem flux model PRELES for varying forest types and climate. *Global Change Biology*, *26*(5), 2923–2943. https://doi.org/10.1111/gcb.14992

Viovy, N. (2018). CRUNCEP version 7—Atmospheric forcing data for the community land model [Dataset]. NCAR. https://doi.org/10.5065/PZ8F-F017

Walther, S., Besnard, S., Nelson, J. A., El-Madany, T. S., Migliavacca, M., Weber, U., et al. (2022a). Technical note: A view from space on global flux towers by MODIS and Landsat: The FluxnetEO dataset (Landsat) [Dataset]. ICOS. https://doi.org/10.18160/0Z7J-J3TR

Walther, S., Besnard, S., Nelson, J. A., El-Madany, T. S., Migliavacca, M., Weber, U., et al. (2022b). Technical note: A view from space on global flux towers by MODIS and Landsat: The FluxnetEO dataset (MODIS) [Dataset]. ICOS. https://doi.org/10.18160/XTV7-WXVZ

Wang, H., Prentice, I. C., Keenan, T. F., Davis, T. W., Wright, I. J., Cornwell, W. K., et al. (2017a). Towards a universal model for carbon dioxide uptake by plants. *Nature Plants*, *3*(9), 734–741. https://doi.org/10.1038/s41477-017-0006-8

Wang, R., Goll, D., Balkanski, Y., Hauglustaine, D., Boucher, O., Ciais, P., et al. (2017b). Global forest carbon uptake due to nitrogen and phosphorus deposition from 1850 to 2100. *Global Change Biology*, *23*(11), 4854–4872. https://doi.org/10.1111/gcb.13766

Wenzel, S., Cox, P. M., Eyring, V., & Friedlingstein, P. (2014). Emergent constraints on climate-carbon cycle feedbacks in the CMIP5 Earth system models. *Journal of Geophysical Research: Biogeosciences*, *119*(5), 794–807. https://doi.org/10.1002/2013jg002591

Xiao, X., Hollinger, D., Aber, J., Goltz, M., Davidson, E. A., Zhang, Q., & Moore, B., III. (2004). Satellite-based modeling of gross primary production in an evergreen needleleaf forest. *Remote Sensing of Environment*, *89*(4), 519–534. https://doi.org/10.1016/j.rse.2003.11.008

Xie, X., & Li, A. (2020). An adjusted two-leaf light use efficiency model for improving GPP simulations over mountainous areas. *Journal of Geophysical Research: Atmospheres*, *125*(13), e2019JD031702. https://doi.org/10.1029/2019jd031702

Xu, T., & Hutchinson, M. (2011). *ANUCLIM version 6.1 user guide* (Vol. 90). The Australian National University, Fenner School of Environment and Society.

Yan, H., Wang, S. Q., Yu, K. L., Wang, B., Yu, Q., Bohrer, G., et al. (2017). A novel diffuse fraction-based two-leaf light use efficiency model: An application quantifying photosynthetic seasonality across 20 AmeriFlux flux tower sites. *Journal of Advances in Modeling Earth Systems*, *9*(6), 2317–2332. https://doi.org/10.1002/2016ms000886

Yuan, W., Cai, W., Liu, S., Dong, W., Chen, J., Arain, M. A., et al. (2014a). Vegetation-specific model parameters are not required for estimating gross primary production. *Ecological Modelling*, *292*, 1–10. https://doi.org/10.1016/j.ecolmodel.2014.08.017

Yuan, W., Cai, W., Xia, J., Chen, J., Liu, S., Dong, W., et al. (2014b). Global comparison of light use efficiency models for simulating terrestrial vegetation gross primary production based on the LaThuile database. *Agricultural and Forest Meteorology*, *192*, 108–120. https://doi.org/10.1016/j.agrformet.2014.03.007

Yuan, W., Liu, S., Zhou, G., Zhou, G., Tieszen, L. L., Baldocchi, D., et al. (2007). Deriving a light use efficiency model from eddy covariance flux data for predicting daily gross primary production across biomes. *Agricultural and Forest Meteorology*, *143*(3–4), 189–207. https://doi.org/10.1016/j.agrformet.2006.12.001

Yuan, W., Zheng, Y., Piao, S., Ciais, P., Lombardozzi, D., Wang, Y., et al. (2019). Increased atmospheric vapor pressure deficit reduces global vegetation growth. *Science Advances*, *5*(8), eaax1396. https://doi.org/10.1126/sciadv.aax1396

Zhang, F., Chen, J. M., Chen, J., Gough, C. M., Martin, T. A., & Dragoni, D. (2012). Evaluating spatial and temporal patterns of MODIS GPP over the conterminous US against flux measurements and a process model. *Remote Sensing of Environment*, *124*, 717–729. https://doi.org/10.1016/j.rse.2012.06.023

Zheng, Y., Shen, R., Wang, Y., Li, X., Liu, S., Liang, S., et al. (2020). Improved estimate of global gross primary production for reproducing its long-term variation, 1982–2017. *Earth System Science Data*, *12*(4), 2725–2746. https://doi.org/10.5194/essd-12-2725-2020

Zheng, Y., Zhang, L., Xiao, J., Yuan, W., Yan, M., Li, T., & Zhang, Z. (2018). Sources of uncertainty in gross primary productivity simulated by light use efficiency models: Model structure, parameters, input data, and spatial resolution. *Agricultural and Forest Meteorology*, *263*, 242–257. https://doi.org/10.1016/j.agrformet.2018.08.003

Zhou, Y., Wu, X., Ju, W., Chen, J. M., Wang, S., Wang, H., et al. (2016). Global parameterization and validation of a two-leaf light use efficiency model for predicting gross primary production across FLUXNET sites. *Journal of Geophysical Research: Biogeosciences*, *121*(4), 1045–1072. https://doi.org/10.1002/2014jg002876

References From the Supporting Information

Acosta, M., Pavelka, M., Montagnani, L., Kutsch, W., Lindroth, A., Juszczak, R., & Janouš, D. (2013). Soil surface CO_2 efflux measurements in Norway spruce forests: Comparison between four different sites across Europe—From boreal to alpine forest. *Geoderma*, *192*, 295–303. https://doi.org/10.1016/j.geoderma.2012.08.027

Ammann, C., Spirig, C., Leifeld, J., & Neftel, A. (2009). Assessment of the nitrogen and carbon budget of two managed temperate grassland fields. *Agriculture, Ecosystems & Environment*, *133*(3), 150–162. https://doi.org/10.1016/j.agee.2009.05.006

Anthoni, P. M., Knohl, A., Rebmann, C., Freibauer, A., Mund, M., Ziegler, W., et al. (2004). Forest and agricultural land-use-dependent CO_2 exchange in Thuringia, Germany. *Global Change Biology*, *10*(12), 2005–2019. https://doi.org/10.1111/j.1365-2486.2004.00863.x

Arain, M. A., & Restrepo-Coupe, N. (2005). Net ecosystem production in a temperate pine plantation in southeastern Canada. *Agricultural and Forest Meteorology*, *128*(3–4), 223–241. https://doi.org/10.1016/j.agrformet.2004.10.003

Archibald, S. A., Kirton, A., van der Merwe, M. R., Scholes, R. J., Williams, C. A., & Hanan, N. (2009). Drivers of inter-annual variability in net ecosystem exchange in a semi-arid savanna ecosystem, South Africa. *Biogeosciences*, *6*(2), 251–266. https://doi.org/10.5194/bg-6-251-2009

Ardö, J., Mölder, M., El-Tahir, B. A., & Elkhidir, H. A. M. (2008). Seasonal variation of carbon fluxes in a sparse savanna in semi arid Sudan. *Carbon Balance and Management*, *3*(1), 7. https://doi.org/10.1186/1750-0680-3-7

Arneth, A., Kurbatova, J., Kolle, O., Shibistova, O. B., Lloyd, J., Vygodskaya, N. N., & Schulze, E. D. (2002). Comparative ecosystem–atmosphere exchange of energy and mass in a European Russian and a central Siberian bog II. Interseasonal and interannual variability of CO_2 fluxes. *Tellus B: Chemical and Physical Meteorology*, *54*(5), 514–530. https://doi.org/10.3402/tellusb.v54i5.16684

Aubinet, M., Moureaux, C., Bodson, B., Dufranne, D., Heinesch, B., Suleau, M., et al. (2009). Carbon sequestration by a crop over a 4-year sugar beet/winter wheat/seed potato/winter wheat rotation cycle. *Agricultural and Forest Meteorology*, *149*(3–4), 407–418. https://doi.org/10.1016/j.agrformet.2008.09.003

Aurela, M., Lohila, A., Tuovinen, J. P., Hatakka, J., Penttila, T., & Laurila, T. (2015). Carbon dioxide and energy flux measurements in four northern-boreal ecosystems at Pallas. *Boreal Environment Research*, *20*(4), 455–473.

Aurela, M., Riutta, T., Laurila, T., Tuovinen, J.-P., Vesala, T., Tuittila, E.-S., et al. (2007). CO_2 exchange of a sedge fen in southern Finland—The impact of a drought period. *Tellus B: Chemical and Physical Meteorology*, *59*(5), 826–837. https://doi.org/10.1111/j.1600-0889.2007.00309.x

Baldocchi, D. D., Vogel, C. A., & Hall, B. (1997). Seasonal variation of carbon dioxide exchange rates above and below a boreal jack pine forest. *Agricultural and Forest Meteorology*, *83*(1–2), 147–170. https://doi.org/10.1016/s0168-1923(96)02335-0

Belelli Marchesini, L., Papale, D., Reichstein, M., Vuichard, N., Tchebakova, N., & Valentini, R. (2007). Carbon balance assessment of a natural steppe of southern Siberia by multiple constraint approach. *Biogeosciences*, *4*(4), 581–595. https://doi.org/10.5194/bg-4-581-2007

Berbigier, P., Bonnefond, J.-M., & Mellmann, P. (2001). CO_2 and water vapour fluxes for 2 years above Euroflux forest site. *Agricultural and Forest Meteorology*, *108*(3), 183–197. https://doi.org/10.1016/S0168-1923(01)00240-4

Bergeron, O., Margolis, H. A., Black, T. A., Coursolle, C., Dunn, A. L., Barr, A. G., & Wofsy, S. C. (2007). Comparison of carbon dioxide fluxes over three boreal black spruce forests in Canada. *Global Change Biology*, *13*(1), 89–107. https://doi.org/10.1111/j.1365-2486.2006.01281.x

Beringer, J., Hacker, J., Hutley, L. B., Leuning, R., Arndt, S. K., Amiri, R., et al. (2011). SPECIAL—Savanna patterns of energy and carbon integrated across the landscape. *Bulletin of the American Meteorological Society*, *92*(11), 1467–1485. https://doi.org/10.1175/2011bams2948.1

Beringer, J., Hutley, L. B., McHugh, I., Arndt, S. K., Campbell, D., Cleugh, H. A., et al. (2016). An introduction to the Australian and New Zealand flux tower network–OzFlux. *Biogeosciences*, *13*(21), 5895–5916. https://doi.org/10.5194/bg-13-5895-2016

Beringer, J., Hutley, L. B., Tapper, N. J., Coutts, A., Kerley, A., & O'Grady, A. P. (2003). Fire impacts on surface heat, moisture and carbon fluxes from a tropical savanna in northern Australia. *International Journal of Wildland Fire*, *12*(4), 333–340. https://doi.org/10.1071/wf03023

Bernhofer, C., Aubinet, M., Clement, R., Grelle, A., Grünwald, T., Ibrom, A., et al. (2003). Spruce forests (Norway and Sitka spruce, including douglas fir): Carbon and water fluxes and balances, ecological and ecophysiological determinants. In R. Valentini (Ed.), *Fluxes of carbon, water and energy of European forests* (pp. 99–123). Springer Berlin Heidelberg.

Besnard, S., Carvalhais, N., Arain, M. A., Black, A., Brede, B., Buchmann, N., et al. (2019). Memory effects of climate and vegetation affecting net ecosystem CO_2 fluxes in global forests. *PLoS One*, *14*(2), e0211510. https://doi.org/10.1371/journal.pone.0211510

Billesbach, D., Bradford, J., & Torn, M. (2016). *FLUXNET2015 US-AR1 ARM USDA UNL OSU woodward switchgrass 1*. FluxNet; Lawerence Berkeley National Lab; US Department of Agriculture; University of Nebraska.

Black, T., Den Hartog, G., Neumann, H., Blanken, P., Yang, P., Russell, C., et al. (1996). Annual cycles of water vapour and carbon dioxide fluxes in and above a boreal aspen forest. *Global Change Biology*, *2*(3), 219–229. https://doi.org/10.1111/j.1365-2486.1996.tb00074.x

Bloomfield, K. J., Cernusak, L. A., Eamus, D., Ellsworth, D. S., Colin Prentice, I., Wright, I. J., et al. (2018). A continental-scale assessment of variability in leaf traits: Within species, across sites and between seasons. *Functional Ecology*, *32*(6), 1492–1506. https://doi.org/10.1111/1365-2435.13097

Boese, S., Jung, M., Carvalhais, N., Teuling, A. J., & Reichstein, M. (2019). Carbon–water flux coupling under progressive drought. *Biogeosciences*, *16*(13), 2557–2572. https://doi.org/10.5194/bg-16-2557-2019

Bowling, D. (2016). *AmeriFlux US-cop corral pocket*. LawrenceBerkeley National Laboratory (LBNL), AmeriFlux; University of Utah.

Bristow, M., Hutley, L. B., Beringer, J., Livesley, S. J., Edwards, A. C., & Arndt, S. K. (2016). Quantifying the relative importance of greenhouse gas emissions from current and future savanna land use change across northern Australia. *Biogeosciences*, *13*(22), 6285–6303. https://doi.org/10.5194/bg-13-6285-2016

Carrara, A., Janssens, I. A., Yuste, J. C., & Ceulemans, R. (2004). Seasonal changes in photosynthesis, respiration and NEE of a mixed temperate forest. *Agricultural and Forest Meteorology*, *126*(1–2), 15–31. https://doi.org/10.1016/j.agrformet.2004.05.002

Chen, S., Chen, J., Lin, G., Zhang, W., Miao, H., Wei, L., et al. (2009). Energy balance and partition in Inner Mongolia steppe ecosystems with different land use types. *Agricultural and Forest Meteorology*, *149*(11), 1800–1809. https://doi.org/10.1016/j.agrformet.2009.06.009

Chiesi, M., Maselli, F., Bindi, M., Fibbi, L., Cherubini, P., Arlotta, E., et al. (2005). Modelling carbon budget of Mediterranean forests using ground and remote sensing measurements. *Agricultural and Forest Meteorology*, *135*(1), 22–34. https://doi.org/10.1016/j.agrformet.2005.09.011

Clark, K. L., Gholz, H. L., Moncrieff, J. B., Cropley, F., & Loescher, H. W. (1999). Environmental controls over net exchanges of carbon dioxide from contrasting Florida ecosystems. *Ecological Applications*, *9*(3), 936–948. https://doi.org/10.1890/1051-0761(1999)009[0936:ECONEO]2.0.CO;2

Cleverly, J., Boulain, N., Villalobos-Vega, R., Grant, N., Faux, R., Wood, C., et al. (2013). Dynamics of component carbon fluxes in a semi-arid Acacia woodland, central Australia. *Journal of Geophysical Research: Biogeosciences*, *118*(3), 1168–1185. https://doi.org/10.1002/jgrg.20101

Cleverly, J., Eamus, D., Van Gorsel, E., Chen, C., Rumman, R., Luo, Q., et al. (2016). Productivity and evapotranspiration of two contrasting semiarid ecosystems following the 2011 global carbon land sink anomaly. *Agricultural and Forest Meteorology*, *220*, 151–159. https://doi.org/10.1016/j.agrformet.2016.01.086

Cook, B. D., Davis, K. J., Wang, W., Desai, A., Berger, B. W., Teclaw, R. M., et al. (2004). Carbon exchange and venting anomalies in an upland deciduous forest in northern Wisconsin, USA. *Agricultural and Forest Meteorology*, *126*(3), 271–295. https://doi.org/10.1016/j.agrformet.2004.06.008

Coursolle, C., Margolis, H., Giasson, M.-A., Bernier, P.-Y., Amiro, B., Arain, M., et al. (2012). Influence of stand age on the magnitude and seasonality of carbon fluxes in Canadian forests. *Agricultural and Forest Meteorology*, *165*, 136–148. https://doi.org/10.1016/j.agrformet.2012.06.011

Da Rocha, H. R., Manzi, A. O., Cabral, O. M., Miller, S. D., Goulden, M. L., Saleska, S. R., et al. (2009). Patterns of water and heat flux across a biome gradient from tropical forest to savanna in Brazil. *Journal of Geophysical Research*, *114*(G1), G00B12. https://doi.org/10.1029/2007jg000640

DeForest, J. L., Noormets, A., McNulty, S. G., Sun, G., Tenney, G., & Chen, J. (2006). Phenophases alter the soil respiration–temperature relationship in an oak-dominated forest. *International Journal of Biometeorology*, *51*(2), 135–144. https://doi.org/10.1007/s00484-006-0046-7

Desai, A. R., Bolstad, P. V., Cook, B. D., Davis, K. J., & Carey, E. V. (2005). Comparing net ecosystem exchange of carbon dioxide between an old-growth and mature forest in the upper Midwest, USA. *Agricultural and Forest Meteorology*, *128*(1), 33–55. https://doi.org/10.1016/j.agrformet.2004.09.005

Dolman, A. J., Moors, E. J., & Elbers, J. A. (2002). The carbon uptake of a mid latitude pine forest growing on sandy soil. *Agricultural and Forest Meteorology*, *111*(3), 157–170. https://doi.org/10.1016/S0168-1923(02)00024-2

Don, A., Rebmann, C., Kolle, O., Scherer-Lorenzen, M., & Schulze, E.-D. (2009). Impact of afforestation-associated management changes on the carbon balance of grassland. *Global Change Biology*, *15*(8), 1990–2002. https://doi.org/10.1111/j.1365-2486.2009.01873.x

Dušek, J., Čížková, H., Stellner, S., Czerný, R., & Květ, J. (2012). Fluctuating water table affects gross ecosystem production and gross radiation use efficiency in a sedge-grass marsh. *Hydrobiologia*, *692*(1), 57–66. https://doi.org/10.1007/s10750-012-0998-z

Epstein, H. E., Calef, M. P., Walker, M. D., Stuart Chapin, F., III., & Starfield, A. M. (2004). Detecting changes in arctic tundra plant communities in response to warming over decadal time scales. *Global Change Biology*, *10*(8), 1325–1334. https://doi.org/10.1111/j.1529-8817.2003.00810.x

Ferréa, C., Zenone, T., Comolli, R., & Seufert, G. (2012). Estimating heterotrophic and autotrophic soil respiration in a semi-natural forest of Lombardy, Italy. *Pedobiologia*, *55*(6), 285–294. https://doi.org/10.1016/j.pedobi.2012.05.001

Flanagan, L. B., Wever, L. A., & Carlson, P. J. (2002). Seasonal and interannual variation in carbon dioxide exchange and carbon balance in a northern temperate grassland. *Global Change Biology*, *8*(7), 599–615. https://doi.org/10.1046/j.1365-2486.2002.00491.x

Flechard, C. R., Oijen, M. V., Cameron, D. R., Vries, W. D., Ibrom, A., Buchmann, N., et al. (2020). Carbon–nitrogen interactions in European forests and semi-natural vegetation–Part 2: Untangling climatic, edaphic, management and nitrogen deposition effects on carbon sequestration potentials. *Biogeosciences*, *17*(6), 1621–1654. https://doi.org/10.5194/bg-17-1621-2020

Fu, P., & Rich, P. M. (1999). Design and implementation of the solar analyst: An arcview extension for modeling solar radiation at landscape scales. In *Paper presented at the proceedings of the nineteenth annual ESRI user conference*.

Galvagno, M., Wohlfahrt, G., Cremonese, E., Rossini, M., Colombo, R., Filippa, G., et al. (2013). Phenology and carbon dioxide source/sink strength of a subalpine grassland in response to an exceptionally short snow season. *Environmental Research Letters*, *8*(2), 025008. https://doi.org/10.1088/1748-9326/8/2/025008

Giasson, M.-A., Coursolle, C., & Margolis, H. A. (2006). Ecosystem-level CO_2 fluxes from a boreal cutover in eastern Canada before and after scarification. *Agricultural and Forest Meteorology*, *140*(1–4), 23–40. https://doi.org/10.1016/j.agrformet.2006.08.001

Gilmanov, T. G., Tieszen, L. L., Wylie, B. K., Flanagan, L. B., Frank, A. B., Haferkamp, M. R., et al. (2005). Integration of CO_2 flux and remotely-sensed data for primary production and ecosystem respiration analyses in the northern great plains: Potential for quantitative spatial extrapolation. *Global Ecology and Biogeography*, *14*(3), 271–292. https://doi.org/10.1111/j.1466-822X.2005.00151.x

Goldstein, A. H., Hultman, N. E., Fracheboud, J. M., Bauer, M. R., Panek, J. A., Xu, M., et al. (2000). Effects of climate variability on the carbon dioxide, water, and sensible heat fluxes above a ponderosa pine plantation in the Sierra Nevada (CA). *Agricultural and Forest Meteorology*, *101*(2), 113–129. https://doi.org/10.1016/S0168-1923(99)00168-9

Gough, C. M., Vogel, C. S., Schmid, H. P., Su, H. B., & Curtis, P. S. (2008). Multi-year convergence of biometric and meteorological estimates of forest carbon storage. *Agricultural and Forest Meteorology*, *148*(2), 158–170. https://doi.org/10.1016/j.agrformet.2007.08.004

Granier, A., Ceschia, E., Damesin, C., Dufrêne, E., Epron, D., Gross, P., et al. (2000). The carbon balance of a young Beech forest. *Functional Ecology*, *14*(3), 312–325. https://doi.org/10.1046/j.1365-2435.2000.00434.x

Griebel, A., Bennett, L. T., Metzen, D., Cleverly, J., Burba, G., & Arndt, S. K. (2016). Effects of inhomogeneities within the flux footprint on the interpretation of seasonal, annual, and interannual ecosystem carbon exchange. *Agricultural and Forest Meteorology*, *221*, 50–60. https://doi.org/10.1016/j.agrformet.2016.02.002

Gu, L., Pallardy, S. G., Yang, B., Hosman, K. P., Mao, J., Ricciuto, D., et al. (2016). Testing a land model in ecosystem functional space via a comparison of observed and modeled ecosystem flux responses to precipitation regimes and associated stresses in a Central U.S. forest. *Journal of Geophysical Research: Biogeosciences*, *121*(7), 1884–1902. https://doi.org/10.1002/2015JG003302

Hao, Y., Baik, J., & Choi, M. (2019). Developing a soil water index-based Priestley–Taylor algorithm for estimating evapotranspiration over East Asia and Australia. *Agricultural and Forest Meteorology*, *279*, 107760. https://doi.org/10.1016/j.agrformet.2019.107760

Heinsch, F. A., Heilman, J. L., McInnes, K. J., Cobos, D. R., Zuberer, D. A., & Roelke, D. L. (2004). Carbon dioxide exchange in a high marsh on the Texas Gulf Coast: Effects of freshwater availability. *Agricultural and Forest Meteorology*, *125*(1), 159–172. https://doi.org/10.1016/j.agrformet.2004.02.007

Henderson-Sellers, B. (1984). A new formula for latent heat of vaporization of water as a function of temperature. *Quarterly Journal of the Royal Meteorological Society*, *110*(466), 1186–1190. https://doi.org/10.1002/qj.49711046626

Hollinger, D. Y., Goltz, S. M., Davidson, E. A., Lee, J. T., Tu, K., & Valentine, H. T. (1999). Seasonal patterns and environmental control of carbon dioxide and water vapour exchange in an ecotonal boreal forest. *Global Change Biology*, *5*(8), 891–902. https://doi.org/10.1046/j.1365-2486.1999.00281.x

Hommeltenberg, J., Schmid, H. P., Drösler, M., & Werle, P. (2014). Can a bog drained for forestry be a stronger carbon sink than a natural bog forest? *Biogeosciences*, *11*(13), 3477–3493. https://doi.org/10.5194/bg-11-3477-2014

Howard, E. A., Gower, S. T., Foley, J. A., & Kucharik, C. J. (2004). Effects of logging on carbon dynamics of a jack pine forest in Saskatchewan, Canada. *Global Change Biology*, *10*(8), 1267–1284. https://doi.org/10.1111/j.1529-8817.2003.00804.x

Humphreys, E. R., Black, T. A., Morgenstern, K., Cai, T., Drewitt, G. B., Nesic, Z., & Trofymow, J. (2006). Carbon dioxide fluxes in coastal Douglas-fir stands at different stages of development after clearcut harvesting. *Agricultural and Forest Meteorology*, *140*(1–4), 6–22. https://doi.org/10.1016/j.agrformet.2006.03.018

Hutley, L. B., Beringer, J., Isaac, P. R., Hacker, J. M., & Cernusak, L. A. (2011). A sub-continental scale living laboratory: Spatial patterns of savanna vegetation over a rainfall gradient in northern Australia. *Agricultural and Forest Meteorology*, *151*(11), 1417–1428. https://doi.org/10.1016/j.agrformet.2011.03.002

Ikawa, H., Nakai, T., Busey, R. C., Kim, Y., Kobayashi, H., Nagai, S., et al. (2015). Understory CO_2, sensible heat, and latent heat fluxes in a black spruce forest in interior Alaska. *Agricultural and Forest Meteorology*, *214–215*, 80–90. https://doi.org/10.1016/j.agrformet.2015.08.247

Imer, D., Merbold, L., Eugster, W., & Buchmann, N. (2013). Temporal and spatial variations of soil CO_2, CH_4 and N_2O fluxes at three differently managed grasslands. *Biogeosciences*, *10*(9), 5931–5945. https://doi.org/10.5194/bg-10-5931-2013

Jacobs, C. M. J., Jacobs, A. F. G., Bosveld, F. C., Hendriks, D. M. D., Hensen, A., Kroon, P. S., et al. (2007). Variability of annual CO_2 exchange from Dutch grasslands. *Biogeosciences*, *4*(5), 803–816. https://doi.org/10.5194/bg-4-803-2007

Jarvis, P., Massheder, J., Hale, S., Moncrieff, J., Rayment, M., & Scott, S. (1997). Seasonal variation of carbon dioxide, water vapor, and energy exchanges of a boreal black spruce forest. *Journal of Geophysical Research*, *102*(D24), 28953–28966. https://doi.org/10.1029/97jd01176

Knohl, A., Schulze, E.-D., Kolle, O., & Buchmann, N. (2003). Large carbon uptake by an unmanaged 250-year-old deciduous forest in Central Germany. *Agricultural and Forest Meteorology*, *118*(3), 151–167. https://doi.org/10.1016/S0168-1923(03)00115-1

Koskinen, M., Minkkinen, K., Ojanen, P., Kämäräinen, M., Laurila, T., & Lohila, A. (2014). Measurements of CO_2 exchange with an automated chamber system throughout the year: Challenges in measuring night-time respiration on porous peat soil. *Biogeosciences*, *11*(2), 347–363. https://doi.org/10.5194/bg-11-347-2014

Krupková, L., Marková, I., Havránková, K., Pokorný, R., Urban, O., Šigut, L., et al. (2017). Comparison of different approaches of radiation use efficiency of biomass formation estimation in Mountain Norway spruce. *Trees*, *31*(1), 325–337. https://doi.org/10.1007/s00468-016-1486-2

Kurbatova, J., Li, C., Varlagin, A., Xiao, X., & Vygodskaya, N. (2008). Modeling carbon dynamics in two adjacent spruce forests with different soil conditions in Russia. *Biogeosciences*, *5*(4), 969–980. https://doi.org/10.5194/bg-5-969-2008

Kwon, H., Law, B. E., Thomas, C. K., & Johnson, B. G. (2018). The influence of hydrological variability on inherent water use efficiency in forests of contrasting composition, age, and precipitation regimes in the Pacific Northwest. *Agricultural and Forest Meteorology*, *249*, 488–500. https://doi.org/10.1016/j.agrformet.2017.08.006

Lafleur, P. M., Roulet, N. T., Bubier, J. L., Frolking, S., & Moore, T. R. (2003). Interannual variability in the peatland-atmosphere carbon dioxide exchange at an ombrotrophic bog. *Global Biogeochemical Cycles*, *17*(2). https://doi.org/10.1029/2002gb001983

Law, B. E., Thornton, P. E., Irvine, J., Anthoni, P. M., & Van Tuyl, S. (2001). Carbon storage and fluxes in ponderosa pine forests at different developmental stages. *Global Change Biology*, *7*(7), 755–777. https://doi.org/10.1046/j.1354-1013.2001.00439.x

Leuning, R., Cleugh, H. A., Zegelin, S. J., & Hughes, D. (2005). Carbon and water fluxes over a temperate Eucalyptus forest and a tropical wet/dry savanna in Australia: Measurements and comparison with MODIS remote sensing estimates. *Agricultural and Forest Meteorology*, *129*(3–4), 151–173. https://doi.org/10.1016/j.agrformet.2004.12.004

Lipson, D. A., Wilson, R. F., & Oechel, W. C. (2005). Effects of elevated atmospheric CO_2 on soil microbial biomass, activity, and diversity in a chaparral ecosystem. *Applied and Environmental Microbiology*, *71*(12), 8573–8580. https://doi.org/10.1128/aem.71.12.8573-8580.2005

López-Ballesteros, A., Serrano-Ortiz, P., Kowalski, A. S., Sánchez-Cañete, E. P., Scott, R. L., & Domingo, F. (2017). Subterranean ventilation of allochthonous CO_2 governs net CO_2 exchange in a semiarid Mediterranean grassland. *Agricultural and Forest Meteorology*, *234–235*, 115–126. https://doi.org/10.1016/j.agrformet.2016.12.021

Loubet, B., Laville, P., Lehuger, S., Larmanou, E., Flechard, C., Mascher, N., et al. (2011). Carbon, nitrogen and Greenhouse gases budgets over a four years crop rotation in northern France. *Plant and Soil*, *343*(1–2), 109–137. https://doi.org/10.1007/s11104-011-0751-9

Lund, M., Falk, J. M., Friborg, T., Mbufong, H. N., Sigsgaard, C., Soegaard, H., & Tamstorf, M. P. (2012). Trends in CO_2 exchange in a high Arctic tundra heath, 2000–2010. *Journal of Geophysical Research*, *117*(G2), G02001. https://doi.org/10.1029/2011JG001901

Ma, S., Baldocchi, D., Wolf, S., & Verfaillie, J. (2016). Slow ecosystem responses conditionally regulate annual carbon balance over 15 years in Californian oak-grass savanna. *Agricultural and Forest Meteorology*, *228–229*, 252–264. https://doi.org/10.1016/j.agrformet.2016.07.016

Ma, S., Baldocchi, D. D., Mambelli, S., & Dawson, T. E. (2011). Are temporal variations of leaf traits responsible for seasonal and inter-annual variability in ecosystem CO_2 exchange? *Functional Ecology*, *25*(1), 258–270. https://doi.org/10.1111/j.1365-2435.2010.01779.x

Marcolla, B., Cescatti, A., Montagnani, L., Manca, G., Kerschbaumer, G., & Minerbi, S. (2005). Importance of advection in the atmospheric CO_2 exchanges of an alpine forest. *Agricultural and Forest Meteorology*, *130*(3), 193–206. https://doi.org/10.1016/j.agrformet.2005.03.006

Marcolla, B., Pitacco, A., & Cescatti, A. (2003). Canopy architecture and turbulence structure in a coniferous forest. *Boundary-Layer Meteorology*, *108*(1), 39–59. https://doi.org/10.1023/A:1023027709805

Merbold, L., Ardö, J., Arneth, A., Scholes, R. J., Nouvellon, Y., de Grandcourt, A., et al. (2009). Precipitation as driver of carbon fluxes in 11 African ecosystems. *Biogeosciences*, *6*(6), 1027–1041. https://doi.org/10.5194/bg-6-1027-2009

Merbold, L., Eugster, W., Stieger, J., Zahniser, M., Nelson, D., & Buchmann, N. (2014). Greenhouse gas budget (CO_2, CH_4 and N_2O) of intensively managed grassland following restoration. *Global Change Biology*, *20*(6), 1913–1928. https://doi.org/10.1111/gcb.12518

Meyer, W., Kondrlovà, E., & Koerber, G. (2015). Evaporation of perennial semi-arid woodland in southeastern Australia is adapted for irregular but common dry periods. *Hydrological Processes*, *29*(17), 3714–3726. https://doi.org/10.1002/hyp.10467

Meyers, T. (2016). *FLUXNET2015 US-Goo Goodwin creek*. FluxNet; NOAA/ARL.

Michelot, A., Eglin, T., Dufrene, E., Lelarge-Trouverie, C., & Damesin, C. (2011). Comparison of seasonal variations in water-use efficiency calculated from the carbon isotope composition of tree rings and flux data in a temperate forest. *Plant, Cell and Environment*, *34*(2), 230–244. https://doi.org/10.1111/j.1365-3040.2010.02238.x

Migliavacca, M., Meroni, M., Manca, G., Matteucci, G., Montagnani, L., Grassi, G., et al. (2009). Seasonal and interannual patterns of carbon and water fluxes of a poplar plantation under peculiar eco-climatic conditions. *Agricultural and Forest Meteorology*, *149*(9), 1460–1476. https://doi.org/10.1016/j.agrformet.2009.04.003

Mkhabela, M., Amiro, B., Barr, A., Black, T., Hawthorne, I., Kidston, J., et al. (2009). Comparison of carbon dynamics and water use efficiency following fire and harvesting in Canadian boreal forests. *Agricultural and Forest Meteorology*, *149*(5), 783–794. https://doi.org/10.1016/j.agrformet.2008.10.025

Monson, R. K., Turnipseed, A. A., Sparks, J. P., Harley, P. C., Scott-Denton, L. E., Sparks, K., & Huxman, T. E. (2002). Carbon sequestration in a high-elevation, subalpine forest. *Global Change Biology*, *8*(5), 459–478. https://doi.org/10.1046/j.1365-2486.2002.00480.x

Myneni, R. B., Ramakrishna, R., Nemani, R., & Running, S. W. (1997). Estimation of global leaf area index and absorbed PAR using radiative transfer models. *IEEE Transactions on Geoscience and Remote Sensing*, *35*(6), 1380–1393. https://doi.org/10.1109/36.649788

Nakai, T., Kim, Y., Busey, R. C., Suzuki, R., Nagai, S., Kobayashi, H., et al. (2013). Characteristics of evapotranspiration from a permafrost black spruce forest in interior Alaska. *Polar Science*, *7*(2), 136–148. https://doi.org/10.1016/j.polar.2013.03.003

Nardino, M., Georgiadis, T., Rossi, F., Ponti, F., Miglietta, F., & Magliulo, V. (2002). Primary productivity and evapotranspiration of a mixed forest. In *Paper presented at the congress CNR-ISA Fo*. Istituto per i Sistemi Agricoli e Forestali del Mediterraneo, Portici.

Noormets, A., Chen, J., & Crow, T. R. (2007). Age-dependent changes in ecosystem carbon fluxes in managed forests in northern Wisconsin, USA. *Ecosystems*, *10*(2), 187–203. https://doi.org/10.1007/s10021-007-9018-y

Noormets, A., McNulty, S. G., Domec, J.-C., Gavazzi, M., Sun, G., & King, J. S. (2012). The role of harvest residue in rotation cycle carbon balance in loblolly pine plantations. Respiration partitioning approach. *Global Change Biology*, *18*(10), 3186–3201. https://doi.org/10.1111/j.1365-2486.2012.02776.x

Nossent, J., & Bauwens, W. (2012). Application of a normalized Nash-Sutcliffe efficiency to improve the accuracy of the Sobol'sensitivity analysis of a hydrological model. In *Paper presented at the EGU general assembly conference abstracts*.

Ouimette, A. P., Ollinger, S. V., Richardson, A. D., Hollinger, D. Y., Keenan, T. F., Lepine, L. C., & Vadeboncoeur, M. A. (2018). Carbon fluxes and interannual drivers in a temperate forest ecosystem assessed through comparison of top-down and bottom-up approaches. *Agricultural and Forest Meteorology*, *256–257*, 420–430. https://doi.org/10.1016/j.agrformet.2018.03.017

Papale, D., Migliavacca, M., Cremonese, E., Cescatti, A., Alberti, G., Balzarolo, M., et al. (2015). Carbon, water and energy fluxes of terrestrial ecosystems in Italy. In R. Valentini & F. Miglietta (Eds.), *The greenhouse gas balance of Italy: An insight on managed and natural terrestrial ecosystems* (pp. 11–45). Springer Berlin Heidelberg.

Pastorello, G., Trotta, C., Canfora, E., Chu, H., Christianson, D., Cheah, Y.-W., et al. (2020). The FLUXNET2015 dataset and the ONEFlux processing pipeline for eddy covariance data. *Scientific Data*, *7*(1), 1–27. https://doi.org/10.1038/s41597-020-0534-3

Peichl, M., & Arain, M. A. (2007). Allometry and partitioning of above-and belowground tree biomass in an age-sequence of white pine forests. *Forest Ecology and Management*, *253*(1–3), 68–80. https://doi.org/10.1016/j.foreco.2007.07.003

Pejam, M., Arain, M., & McCaughey, J. (2006). Energy and water vapour exchanges over a mixedwood boreal forest in Ontario, Canada. *Hydrological Processes*, *20*(17), 3709–3724. https://doi.org/10.1002/hyp.6384

Pereira, J. S., Mateus, J. A., Aires, L. M., Pita, G., Pio, C., David, J. S., et al. (2007). Net ecosystem carbon exchange in three contrasting Mediterranean ecosystems—The effect of drought. *Biogeosciences*, *4*(5), 791–802. https://doi.org/10.5194/bg-4-791-2007

Perez-Priego, O., El-Madany, T. S., Migliavacca, M., Kowalski, A. S., Jung, M., Carrara, A., et al. (2017). Evaluation of eddy covariance latent heat fluxes with independent lysimeter and sapflow estimates in a Mediterranean savannah ecosystem. *Agricultural and Forest Meteorology*, *236*, 87–99. https://doi.org/10.1016/j.agrformet.2017.01.009

Pilegaard, K., & Ibrom, A. (2020). Net carbon ecosystem exchange during 24 years in the Sorø Beech Forest–relations to phenology and climate. *Tellus B: Chemical and Physical Meteorology*, *72*(1), 1–17. https://doi.org/10.1080/16000889.2020.1822063

Poggio, L., de Sousa, L. M., Batjes, N. H., Heuvelink, G. B. M., Kempen, B., Ribeiro, E., & Rossiter, D. (2021). SoilGrids 2.0: Producing soil information for the globe with quantified spatial uncertainty. *Soil*, *7*(1), 217–240. https://doi.org/10.5194/soil-7-217-2021

Powell, T. L., Bracho, R., Li, J., Dore, S., Hinkle, C. R., & Drake, B. G. (2006). Environmental controls over net ecosystem carbon exchange of scrub oak in central Florida. *Agricultural and Forest Meteorology*, *141*(1), 19–34. https://doi.org/10.1016/j.agrformet.2006.09.002

Prescher, A.-K., Grünwald, T., & Bernhofer, C. (2010). Land use regulates carbon budgets in eastern Germany: From NEE to NBP. *Agricultural and Forest Meteorology*, *150*(7), 1016–1025. https://doi.org/10.1016/J.AGRFORMET.2010.03.008

Priestley, C. H. B., & Taylor, R. (1972). On the assessment of surface heat flux and evaporation using large-scale parameters. *Monthly Weather Review*, *100*(2), 81–92. https://doi.org/10.1175/1520-0493(1972)100<0081:otaosh>2.3.co;2

Rambal, S., Joffre, R., Ourcival, J. M., Cavender-Bares, J., & Rocheteau, A. (2004). The growth respiration component in eddy CO_2 flux from a Quercus ilex mediterranean forest. *Global Change Biology*, *10*(9), 1460–1469. https://doi.org/10.1111/j.1365-2486.2004.00819.x

Rebmann, C., Zeri, M., Lasslop, G., Mund, M., Kolle, O., Schulze, E.-D., & Feigenwinter, C. (2010). Treatment and assessment of the CO_2-exchange at a complex forest site in Thuringia, Germany. *Agricultural and Forest Meteorology*, *150*(5), 684–691. https://doi.org/10.1016/j.agrformet.2009.11.001

Reichstein, M., Falge, E., Baldocchi, D., Papale, D., Aubinet, M., Berbigier, P., et al. (2005). On the separation of net ecosystem exchange into assimilation and ecosystem respiration: Review and improved algorithm. *Global Change Biology*, *11*(9), 1424–1439. https://doi.org/10.1111/j.1365-2486.2005.001002.x

Renchon, A. A., Griebel, A., Metzen, D., Williams, C. A., Medlyn, B., Duursma, R. A., et al. (2018). Upside-down fluxes Down Under: CO_2 net sink in winter and net source in summer in a temperate evergreen broadleaf forest. *Biogeosciences*, *15*(12), 3703–3716. https://doi.org/10.5194/bg-15-3703-2018

Reverter, B. R., Sánchez-Cañete, E. P., Resco, V., Serrano-Ortiz, P., Oyonarte, C., & Kowalski, A. S. (2010). Analyzing the major drivers of NEE in a Mediterranean alpine shrubland. *Biogeosciences*, *7*(9), 2601–2611. https://doi.org/10.5194/bg-7-2601-2010

Rey, A., Pegoraro, E., Tedeschi, V., De Parri, I., Jarvis, P. G., & Valentini, R. (2002). Annual variation in soil respiration and its components in a coppice oak forest in Central Italy. *Global Change Biology*, *8*(9), 851–866. https://doi.org/10.1046/j.1365-2486.2002.00521.x

Rodrigues, A., Pita, G., Mateus, J., Kurz-Besson, C., Casquilho, M., Cerasoli, S., et al. (2011). Eight years of continuous carbon fluxes measurements in a Portuguese eucalypt stand under two main events: Drought and felling. *Agricultural and Forest Meteorology*, *151*(4), 493–507. https://doi.org/10.1016/j.agrformet.2010.12.007

Roman, D. T., Novick, K. A., Brzostek, E. R., Dragoni, D., Rahman, F., & Phillips, R. P. (2015). The role of isohydric and anisohydric species in determining ecosystem-scale response to severe drought. *Oecologia*, *179*(3), 641–654. https://doi.org/10.1007/s00442-015-3380-9

Rouse, J. W., Haas, R. H., Schell, J. A., Deering, D. W., & Harlan, J. C. (1974). *Monitoring the vernal advancement and retrogradation (green wave effect) of natural vegetation* (p. 371). NASA/GSFC Type III Final Report.

Ruehr, N. K., Law, B. E., Quandt, D., & Williams, M. (2014). Effects of heat and drought on carbon and water dynamics in a regenerating semi-arid pine forest: A combined experimental and modeling approach. *Biogeosciences*, *11*(15), 4139–4156. https://doi.org/10.5194/bg-11-4139-2014

Running, S. W., & Zhao, M. (2015). *Daily GPP and annual NPP (MOD17A2/A3) products NASA Earth Observing System MODIS land algorithm*. MOD17 User's Guide.

Sabbatini, S., Arriga, N., Bertolini, T., Castaldi, S., Chiti, T., Consalvo, C., et al. (2016). Greenhouse gas balance of cropland conversion to bioenergy poplar short-rotation coppice. *Biogeosciences*, *13*(1), 95–113. https://doi.org/10.5194/bg-13-95-2016

Sagerfors, J., Lindroth, A., Grelle, A., Klemedtsson, L., Weslien, P., & Nilsson, M. (2008). Annual CO_2 exchange between a nutrient-poor, minerotrophic, boreal mire and the atmosphere. *Journal of Geophysical Research*, *113*(G1), G01001. https://doi.org/10.1029/2006JG000306

Sanz, M. J., Carrara, A., Gimeno, C., Bucher, A., & Lopez, R. (2004). Effects of a dry and warm summer conditions on CO_2 and energy fluxes from three Mediterranean ecosystems. In *Paper presented at the geophysics Research Abstracts*.

Savitzky, A., & Golay, M. J. (1964). Smoothing and differentiation of data by simplified least squares procedures. *Analytical Chemistry*, *36*(8), 1627–1639. https://doi.org/10.1021/ac60214a047

Schaaf, C., & Wang, Z. (2015). MCD43A4 MODIS/Terra+ Aqua BRDF/Albedo Nadir BRDF adjusted ref daily L3 global-500m V006 [Dataset]. NASA EOSDIS Land Processes DAAC. https://earthexplorer.usgs.gov

Schroder, I. (2014). Arcturus Emerald OzFlux tower site OzFlux: Australian and New Zealand flux research and monitoring. *hdl*, *102*(100), 14249.

Scott, R. L. (2010). Using watershed water balance to evaluate the accuracy of eddy covariance evaporation measurements for three semiarid ecosystems. *Agricultural and Forest Meteorology*, *150*(2), 219–225. https://doi.org/10.1016/j.agrformet.2009.11.002

Scott, R. L., Biederman, J. A., Hamerlynck, E. P., & Barron-Gafford, G. A. (2015). The carbon balance pivot point of southwestern U.S. semiarid ecosystems: Insights from the 21st century drought. *Journal of Geophysical Research: Biogeosciences*, *120*(12), 2612–2624. https://doi.org/10.1002/2015JG003181

Scott, R. L., Jenerette, G. D., Potts, D. L., & Huxman, T. E. (2009). Effects of seasonal drought on net carbon dioxide exchange from a woody-plant-encroached semiarid grassland. *Journal of Geophysical Research*, *114*(G4), G04004. https://doi.org/10.1029/2008JG000900

Serrano-Ortiz, P., Domingo, F., Cazorla, A., Were, A., Cuezva, S., Villagarcía, L., et al. (2009). Interannual CO_2 exchange of a sparse Mediterranean shrubland on a carbonaceous substrate. *Journal of Geophysical Research*, *114*(G4), G04015. https://doi.org/10.1029/2009JG000983

Shi, P., Sun, X., Xu, L., Zhang, X., He, Y., Zhang, D., & Yu, G. (2006). Net ecosystem CO_2 exchange and controlling factors in a steppe—Kobresia meadow on the Tibetan Plateau. *Science in China—Series D: Earth Sciences*, *49*(2), 207–218. https://doi.org/10.1007/s11430-006-8207-4

Sulman, B. N., Desai, A. R., Cook, B. D., Saliendra, N., & Mackay, D. S. (2009). Contrasting carbon dioxide fluxes between a drying shrub wetland in Northern Wisconsin, USA, and nearby forests. *Biogeosciences*, *6*(6), 1115–1126. https://doi.org/10.5194/bg-6-1115-2009

Suni, T., Rinne, J., Reissell, A., Altimir, N., Keronen, P., Rannik, U., et al. (2003). Long-term measurements of surface fluxes above a Scots pine forest in Hyytiala, southern Finland, 1996-2001. *Boreal Environment Research*, *8*(4), 287–301.

Syed, K. H., Flanagan, L. B., Carlson, P. J., Glenn, A. J., & Van Gaalen, K. E. (2006). Environmental control of net ecosystem CO_2 exchange in a treed, moderately rich fen in northern Alberta. *Agricultural and Forest Meteorology*, *140*(1–4), 97–114. https://doi.org/10.1016/j.agrformet.2006.03.022

Tang, B., Zhao, X., & Zhao, W. (2018). Local effects of forests on temperatures across Europe. *Remote Sensing*, *10*(4), 529. https://doi.org/10.3390/rs10040529

Tang, X., Zhou, Y., Li, H., Yao, L., Ding, Z., Ma, M., & Yu, P. (2020). Remotely monitoring ecosystem respiration from various grasslands along a large-scale east–west transect across northern China. *Carbon Balance and Management*, *15*, 1–14. https://doi.org/10.1186/s13021-020-00141-8

Tatarinov, F., Rotenberg, E., Maseyk, K., Ogée, J., Klein, T., & Yakir, D. (2016). Resilience to seasonal heat wave episodes in a Mediterranean pine forest. *New Phytologist*, *210*(2), 485–496. https://doi.org/10.1111/nph.13791

Tedeschi, V., Rey, A., Manca, G., Valentini, R., Jarvis, P. G., & Borghetti, M. (2006). Soil respiration in a Mediterranean oak forest at different developmental stages after coppicing. *Global Change Biology*, *12*(1), 110–121. https://doi.org/10.1111/j.1365-2486.2005.01081.x

Thomas, C. K., Law, B. E., Irvine, J., Martin, J. G., Pettijohn, J. C., & Davis, K. J. (2009). Seasonal hydrology explains interannual and seasonal variation in carbon and water exchange in a semiarid mature ponderosa pine forest in central Oregon. *Journal of Geophysical Research*, *114*(G4), G04006. https://doi.org/10.1029/2009JG001010

Thum, T., Aalto, T., Laurila, T., Aurela, M., Kolari, P., & Hari, P. (2007). Parametrization of two photosynthesis models at the canopy scale in a northern boreal Scots pine forest. *Tellus Series B Chemical and Physical Meteorology*, *59*(5), 874–890. https://doi.org/10.1111/j.1600-0889.2007.00305.x

Tirone, G., Dore, S., Matteucci, G., Greco, S., & Valentini, R. (2003). Evergreen Mediterranean forests. Carbon and water fluxes, balances, ecological and ecophysiological determinants. In R. Valentini (Ed.), *Fluxes of carbon, water and energy of European forests* (pp. 125–149). Springer Berlin Heidelberg.

Tramontana, G., Jung, M., Schwalm, C. R., Ichii, K., Camps-Valls, G., Ráduly, B., et al. (2016). Predicting carbon dioxide and energy fluxes across global FLUXNET sites with regression algorithms. *Biogeosciences*, *13*(14), 4291–4313. https://doi.org/10.5194/bg-13-4291-2016

Trautmann, T., Koirala, S., Caryalhais, N., Eicker, A., Finks, M., Niemann, C., & Jung, M. (2018). Understanding terrestrial water storage variations in northern latitudes across scales. *Hydrology and Earth System Sciences*, *22*(7), 4061–4082. https://doi.org/10.5194/hess-22-4061-2018

Turner, D., Ritts, W., Styles, J., Yang, Z., Cohen, W., Law, B., & Thornton, P. (2006). A diagnostic carbon flux model to monitor the effects of disturbance and interannual variation in climate on regional NEP. *Tellus B: Chemical and Physical Meteorology*, *58*(5), 476–490. https://doi.org/10.3402/tellusb.v58i5.17028

Ulke, A. G., Gattinoni, N. N., & Posse, G. (2015). Analysis and modelling of turbulent fluxes in two different ecosystems in Argentina. *International Journal of Environment and Pollution*, *58*(1–2), 52–62. https://doi.org/10.1504/ijep.2015.076583

Urbanski, S., Barford, C., Wofsy, S., Kucharik, C., Pyle, E., Budney, J., et al. (2007). Factors controlling CO_2 exchange on timescales from hourly to decadal at Harvard Forest. *Journal of Geophysical Research*, *112*(G2), G02020. https://doi.org/10.1029/2006JG000293

Valentini, R., De Angelis, P., Matteucci, G., Monaco, R., Dore, S., & Mucnozza, G. E. S. (1996). Seasonal net carbon dioxide exchange of a beech forest with the atmosphere. *Global Change Biology*, *2*(3), 199–207. https://doi.org/10.1111/j.1365-2486.1996.tb00072.x

Valentini, R., Matteucci, G., Dolman, A. J., Schulze, E. D., Rebmann, C., Moors, E. J., et al. (2000). Respiration as the main determinant of carbon balance in European forests. *Nature*, *404*(6780), 861–865. https://doi.org/10.1038/35009084

Veenendaal, E. M., Kolle, O., & Lloyd, J. (2004). Seasonal variation in energy fluxes and carbon dioxide exchange for a broad-leaved semi-arid savanna (Mopane woodland) in Southern Africa. *Global Change Biology*, *10*(3), 318–328. https://doi.org/10.1111/j.1365-2486.2003.00699.x

Vickers, D., Thomas, C., Pettijohn, C., Martin, J. G., & Law, B. (2012). Five years of carbon fluxes and inherent water-use efficiency at two semi-arid pine forests with different disturbance histories. *Tellus B: Chemical and Physical Meteorology*, *64*(1), 17159. https://doi.org/10.3402/tellusb.v64i0.17159

Viovy, N. (2018). CRUNCEP version 7—Atmospheric forcing data for the community land model. https://doi.org/10.5065/PZ8F-F017

Vitale, L., Di Tommasi, P., D'Urso, G., & Magliulo, V. (2016). The response of ecosystem carbon fluxes to LAI and environmental drivers in a maize crop grown in two contrasting seasons. *International Journal of Biometeorology*, *60*(3), 411–420. https://doi.org/10.1007/s00484-015-1038-2

Walther, S., Besnard, S., Nelson, J. A., El-Madany, T. S., Migliavacca, M., Weber, U., et al. (2022). Technical note: A view from space on global flux towers by MODIS and Landsat: The FluxnetEO data set. *Biogeosciences*, *19*(11), 2805–2840. https://doi.org/10.5194/bg-19-2805-2022

Weiss, A., & Norman, J. (1985). Partitioning solar radiation into direct and diffuse, visible and near-infrared components. *Agricultural and Forest Meteorology*, *34*(2–3), 205–213. https://doi.org/10.1016/0168-1923(85)90020-6

Wharton, S., Falk, M., Bible, K., Schroeder, M., & Paw U, K. T. (2012). Old-growth CO_2 flux measurements reveal high sensitivity to climate anomalies across seasonal, annual and decadal time scales. *Agricultural and Forest Meteorology*, *161*, 1–14. https://doi.org/10.1016/j.agrformet.2012.03.007

Williams, M., Law, B. E., Anthoni, P. M., & Unsworth, M. H. (2001). Use of a simulation model and ecosystem flux data to examine carbon–water interactions in ponderosa pine. *Tree Physiology*, *21*(5), 287–298. https://doi.org/10.1093/treephys/21.5.287

Wohlfahrt, G., Hammerle, A., Haslwanter, A., Bahn, M., Tappeiner, U., & Cernusca, A. (2008). Seasonal and inter-annual variability of the net ecosystem CO_2 exchange of a temperate mountain grassland: Effects of weather and management. *Journal of Geophysical Research*, *113*(D8), D08110. https://doi.org/10.1029/2007jd009286

Wolf, S., Eugster, W., Ammann, C., Häni, M., Zielis, S., Hiller, R., et al. (2013). Contrasting response of grassland versus forest carbon and water fluxes to spring drought in Switzerland. *Environmental Research Letters*, *8*(3), 035007. https://doi.org/10.1088/1748-9326/8/3/035007

Yee, M. S., Pauwels, V. R., Daly, E., Beringer, J., Rüdiger, C., McCabe, M. F., & Walker, J. P. (2015). A comparison of optical and microwave scintillometers with eddy covariance derived surface heat fluxes. *Agricultural and Forest Meteorology*, *213*, 226–239. https://doi.org/10.1016/j.agrformet.2015.07.004

Zhang, J.-H., Han, S.-J., & Yu, G.-R. (2006). Seasonal variation in carbon dioxide exchange over a 200-year-old Chinese broad-leaved Korean pine mixed forest. *Agricultural and Forest Meteorology*, *137*(3), 150–165. https://doi.org/10.1016/j.agrformet.2006.02.004

Zielis, S., Etzold, S., Zweifel, R., Eugster, W., Haeni, M., & Buchmann, N. (2014). NEP of a Swiss subalpine forest is significantly driven not only by current but also by previous year's weather. *Biogeosciences*, *11*(6), 1627–1635. https://doi.org/10.5194/bg-11-1627-2014